Managing subfloor moisture, corrosion and insulation performance

Stephen McNeil, Zhengwei Li, Ian Cox-Smith and Nick Marston

1222 Moonshine Rd
RD1, Porirua 5381
Private Bag 50 908
Porirua 5240
New Zealand
branz.nz

Acknowledgements

Managing subfloor moisture, corrosion and insulation performance

BRANZ Study Report SR354

Authors

Stephen McNeil, Zhengwei Li, Ian Cox-Smith and Nick Marston

Reference

Abstract

Many New Zealand buildings are standing on a suspended timber floor, and consequently, there are concerns when it comes to dealing with moisture in this space and the effect on fastener corrosion, timber moisture content and insulation performance.

A field survey was completed on eight homes around New Zealand, measuring and monitoring the framing moisture content, air relative humidity and temperature for a calendar year. Corrosion samples were also installed to assess the corrosivity of the environment relative to atmospheric conditions in multiple places under each building.

In general, the subfloor environment was found to be more benign from the corrosion point of view compared with atmospheric conditions. However, corrosion samples located near vent openings were found to suffer more degradation than the rest of the samples. This is mainly due to greater temperature variation and localised wetting due to rain.

In regards to managing moisture, experimental facilities on site at BRANZ were used to assess the effect of ventilation and ground covering on the accumulation of moisture. The importance of the role that ventilation plays was reaffirmed, with a lack of vents causing a rapid accumulation of moisture in structural framing members. The existing acceptable solution of 3,500 mm^2/m^2 gives additional drying capacity, which provides a reasonable safety margin, although it must be stressed that the research buildings under investigation here were very well exposed and consequently had a higher achieved ventilation rate than what is likely in a suburban environment.

The effectiveness of polythene ground covers was tested, and where they are able to be used, they are an effective means for control of ground-sourced moisture. A

polythene barrier can be difficult to install in many situations, particularly in older buildings. Where they are used, they should be detailed so that they do not provide a space for rainwater to accumulate.

The observed patterns of moisture accumulation indicate that the southern side of a building is more likely to suffer moisture issues and that any inspection or judgement made on the subfloor of a building should consider the entire space and not just the area in the vicinity of the subfloor access.

There have been concerns for wind wash potentially undermining insulation performance. These have been quantified, and a very exposed subfloor will not suffer significant degradation of thermal performance provided a medium-density bulk insulation product is used. In cases where lower-density products are used, upgrading installed R-value by 25% will safeguard against excessive energy loss. In unexposed cases, where ventilation openings are at Building Code specifications, wind wash is insignificant in bulk insulants.

This work also verified the performance (or lack thereof) of draped foil insulation, particularly when it was windy or relatively cold, demonstrating that bulk insulation products are superior.

Keywords

Subfloor, ventilation, infiltration, moisture, corrosion, insulation, wind wash, moisture removal

Contents

Figures

Tables

1.   Introduction

In buildings with a suspended timber floor, the subfloor void or crawl space can be considered the engine room of the home. Previous work at BRANZ established that up to 40 L/day of water vapour can evaporate from the ground into the air in this space. If this is not controlled with ventilation or other means, it can have a major effect on the building and occupants above. This includes accumulation of moisture in building components and effects on corrosion and insulation performance.

This project examines the impact of different mitigation strategies on the moisture levels in the air and building components in the subfloor space of a building with a suspended timber floor. This building was on a well exposed location at the BRANZ site in Judgeford, and strategies applied consisted of ventilation, along with the option to apply a polythene ground barrier on top of the subfloor soil. Various levels of ventilation opening were applied to the building from effectively none through to the New Zealand Building Code clause E2 *External moisture* Acceptable Solution (E2/AS1) for subfloor ventilation of suspended timber floors. This requires a minimum of 3,500 mm^2 of net open area for every 1 m^2 of floor area. The ventilation rates achieved were measured using tracer gas techniques, and timber moisture content, relative humidity and temperature at numerous locations in the space were recorded. A field survey of eight homes around New Zealand was also completed where actual installed ventilation openings were measured, and the temperature, timber moisture content and relative humidity were recorded for a calendar year. Corrosivity specimens were installed under these homes, both in free air and sandwiched between timber blocks, with additional control samples placed with the weatherstations located alongside each house. Corrosivity of the subfloor environment was compared to the atmospheric conditions for each location.

Also examined in the project are two aspects of insulation performance, the effect of wind wash on degradation of effectiveness of a range of insulation products and the impact of moisture on the performance of thermal insulation. Since the role of insulation is to resist the flow of heat, a concern in maintaining performance is the effect of wind undermining this my removing warm air from the insulation product itself, which is termed 'wind wash'. Concerns have been raised as to the scale of this effect, particularly in exposed subfloor situations, but also in respect to the effect of increasing ventilation levels to counteract moisture issues in the subfloor space.

2.   Project structure

This research project was divided into three distinct areas of subfloor performance:

- Corrosion potential of fixing and fasteners.
- Moisture accumulation in framing timber and air.
- Thermal performance factors, whether from moisture accumulation or wind wash undermining insulation performance.

Each area had its own experimental programme and areas where data could be shared between the streams of the project. Work began with a literature review[1] followed by the commissioning of experimental works, allowing subsequent analysis of data and computer modelling to take place.

---

[1] This is an internal BRANZ review titled *Literature Review Report – Subfloor and Roof – March 2014.*

3. Experimental methods

3.1 Field survey

3.1.1 Methodology

To acquire an understanding of environmental conditions in subfloors of typical New Zealand residential houses, BRANZ recruited eight houses – three from Auckland, three from Wellington and two from Invercargill and installed instruments to collect required information for a period of 12 months. See Appendix A for house details.

The monitoring was composed of several parts:

- **Surrounding atmospheric environment:** A portable weatherstation was installed to collect climatic factors including ambient temperature, humidity, rainfall, wind speed and wind direction. The data was recorded every hour.
- **Subfloor environment:** iButton (DS1923) sensors were installed at different locations of a subfloor space to monitor temperature and humidity. Several sensors were also specially arranged to monitor moisture transfer/evaporation from ground soil to subfloor atmosphere (Figure 1). The data was collected every hour. Stainless steel pins were inserted into H3.2 CCA-treated timber blocks (150 × 90 × 45 mm) to measure moisture content of timbers used in subfloor space through an electrical resistance measurement approach. This data was collected every 15 minutes.
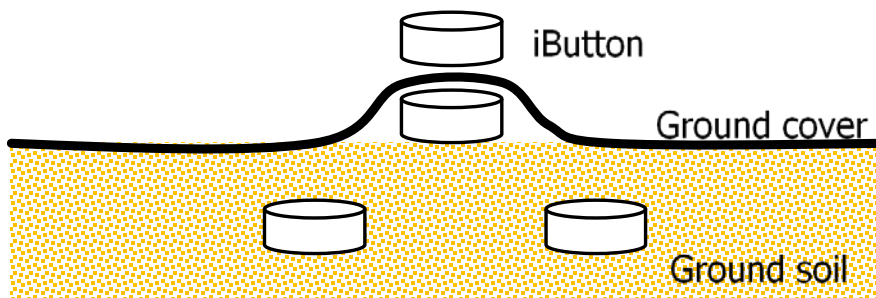
Figure 1. Schematic of sensor (iButton) arrangement for monitoring moisture transfer/evaporation from covered ground in subfloor.

- **Indoor environment:** Two sensors were placed in either the living room or kitchen to monitor changes in indoor temperature and humidity. Two were used for a measure of redundancy. The console of the weatherstation also recorded indoor temperature and humidity every hour where it was installed and was then placed in the kitchen.
- **Corrosivity of subfloor atmosphere:** Precleaned mild steel samples were installed to investigate the aggressiveness of the subfloor environment. This included one set of samples directly exposed to subfloor air and another set sandwiched between the two H3.2 CCA-treated timber blocks where the moisture content was measured (Figure 2).
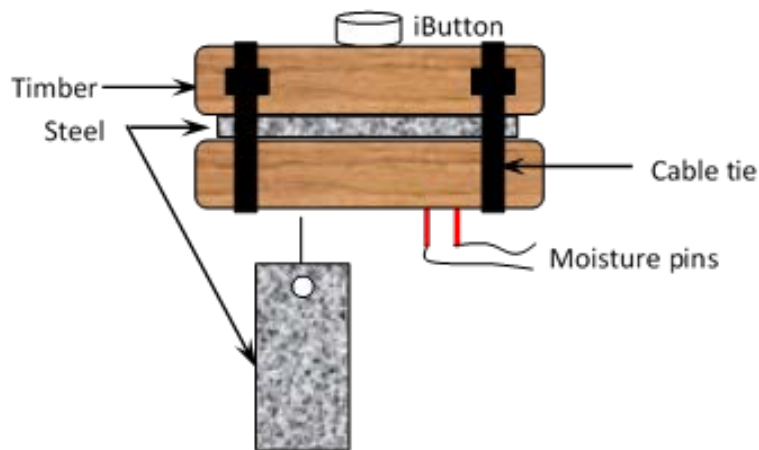
Figure 2. Sample arrangement for subfloor corrosivity measurement.

- **Corrosivity of surrounding atmospheric environment:** Two precleaned mild steel samples were exposed to open atmosphere alongside the weatherstation at an angle of 45° facing towards the north. The mass loss after 12 months was used to classify atmospheric corrosivity.

Appendix A contains details of each house surveyed, including subfloor construction, configuration, dimension, ventilation (number, location and size of vent), ground condition and testing sample arrangement.

3.1.2   Subfloor corrosivity

In New Zealand, around 80% of residential dwellings have suspended timber ground floors. The subfloor is unique simply because it is shielded from rain, water flow, and/or solar irradiation. The ground soil condition could be highly variable depending on the level of the underground water table. Air movement in the subfloor space might be limited compared with open atmosphere. However, it is heavily dependent upon the exact type of construction and ventilation provided. As such, moisture from various sources could have very different ways of movement and lifetimes, for example, depending on the level of ventilation provided, diffusion-driven moisture movement may dominate in some cases.

A variety of materials are used for the construction of subfloors. These typically include timber, concrete and steel. Performance and durability of these materials are essential to the structural stability of the subfloor structure and the performance/safety of the timber-framed building above.

In the 1990s, BRANZ performed a survey of a limited number of houses in the Wellington area to investigate potential correlations between subfloor metal corrosion and the following items:

- Age of fasteners.
- Distance of the house from the sea.
- Level of subfloor ventilation (ingress of airborne sea salt and subfloor humidity).

This study found no clear correlation between distance from the sea and extent of subfloor fastener corrosion. This was probably because there were too many other interfering variables involved, such as type of subfloor construction, age of house, surface protection of metallic component and height of the component from ground.

Performance evaluation was scored qualitatively from 1 to 10 in this survey. This approach had serious limitations since it could not determine the material degradation kinetics. Another factor that could have been obscuring a trend was any variation in the thickness and quality of galvanising over the years separating the ages of the houses inspected.

Therefore, part of the present research is concentrated on corrosion performance evaluation of using controlled metal samples exposed to subfloor atmosphere.

3.1.3   Experimental set-up

Mild steel samples with a dimension of ~120 × 80 × 0.95 mm were cut from cold-rolled sheets. The surface was as originally rolled without further treatment. To measure the corrosivity of the subfloor environment, one set of steel samples was directly exposed to subfloor atmosphere at several (6–7) locations, typically at four corners, two close to vents and one in the centre. The mass loss after 12 months of exposure was measured to calculate mean corrosion rate. Another set of steel samples was placed between two H3.2 CCA-treated timber blocks (~150 × 90 × 45 mm) tightened with two cable ties (Figure 3). This sample configuration was used to simulate corrosion of metal fasteners in timbers. In addition, two steel samples were exposed to the atmosphere directly surrounding the house being surveyed. Their mass losses after 12 months could be used to classify atmospheric corrosivity according to relevant ISO and national standards.

Figure 3. A typical sample set for subfloor (left) and open atmosphere (right) corrosivity measurement.

3.2   Ventilation research building

Figure 4. BRANZ ventilation research building – before enclosing subfloor.

Figure 5. BRANZ ventilation research building – subfloor enclosed with access door open.

3.2.1   Description

The building shown in Figure 4 and Figure 5 was constructed as a prebuilt shell in 2007 and transported onto the research site for the Weathertightness, Air quality and Ventilation Engineering (WAVE) research programme. The single-storey building has a floor area of 91 m^2. The building is a traditional timber-framed construction that is clad with painted fibre-cement weatherboard directly fixed over a flexible wall underlay. The gable roof has corrugated steel cladding on timber trusses. The floor is made of particleboard, which is sealed with polyurethane. The walls and the ceiling are insulated to the requirements of the Building Code with fibreglass batts. All inner wall surfaces and the ceiling are lined with gypsum-based plasterboard, which received three coats of an acrylic paint.

For the purpose of the WAVE ventilation research, the building was fitted with sealable ports that penetrate the envelope. The ports are located in the floor, walls and ceiling connecting the living area to the subfloor, cavity of the outer walls and attic respectively. Our aim was to reach an airtightness level as low as 1 ach @ 50 Pa (all ports sealed) and an upper level of about 9 ach @ 50 Pa (all ports open).

The building was used for ventilation research for 2 years before the start of the subfloor research programme. Prior to this, the subfloor was exposed (Figure 4). It was enclosed in early 2013 (Figure 5) before the onsite measurements started later that year.

3.2.2   Adjustable ventilation openings

The perimeter lining of the subfloor was fitted with a set of 10 steel plates covering penetrations in the plywood enclosure. These were gasketed with closed-cell foam rubber and were interchangeable, which enabled the installation of vents up to a maximum size of 200 mm diameter (Figure 6).

Figure 6. Subfloor vent.

7

3.2.3   Airtightness/leakage area

Airtightness of the subfloor space was tested using BRANZ's Retrotec blower door with the subfloor configured in its most airtight state. A custom cowl and flange (Figure 7) were made that enabled connection of the blower door to the side of the subfloor enclosure.

A blower door allows measurements of air leakage through the building envelope to be made via pressurisation/depressurisation of the internal volume. This is achieved by measuring the flow through a calibrated orifice while a fan maintains a constant pressure across the envelope. Flow rates are measured for a range of pressures across the envelope before a curve fit to the data points is used to obtain a measurement of airtightness. A detailed description of the blower door technique can be found in Jensen (1986).

Figure 7. Blower door cowl and flange.

An additional check was made to ascertain the amount of leakage across the floor of the building using a secondary fan and laminar flow element (LFE). This was used to balance the pressure across the floor diaphragm. Using the two flow rates, the leakage area of the floor was able to be calculated. It was found to be negligible in respect to the leakage opening around the subfloor perimeter. There may well have been flank leakage behind the wall linings and into the roof cavity, but this was not investigated further due to the difficulty of pressurising the highly permeable ceiling cavity.

3.2.4   Instrumentation

The subfloor was instrumented to allow the measurement of temperature, humidity, timber moisture content and tracer gas concentrations in the space. The building was also instrumented for the purposes of the WAVE ventilation project, which gave a very good picture of conditions in the building.

Equipment included the following:

- Agilent 34980 multiplexer with custom reference block for increased thermocouple accuracy.
- Custom relay multiplexer for applying a known voltage to moisture pins for moisture content measurements.
- Edinburgh Instruments dual-beam infrared gascard for N20 tracer decay experiments.
- Innova 1412 photo acoustic gas analyser for longer term infiltration measurements. This was equipped with filters to detect CO_2, Freon 134a and sulphur hexafluoride (SF_6) with detection limits of 3.4 ppm, 0.02 ppm and 0.006 ppm respectively. The dynamic range of this gas monitor is typically 4–5 orders of magnitude.
- BRANZ heat flux sensors.

The equipment was controlled and data collected using the in-house BRANZ data acquisition software FlexiDAQ (Figure 8). FlexiDAQ is a modular system that allows multiple types of instrumentation to be controlled by the same computer using a plugin architecture. In the case of the subfloor research building (Figure 12), indoor sensors were replaced with sensors in the subfloor space. Also, indoor climate control or the ventilation system did not apply in this project.
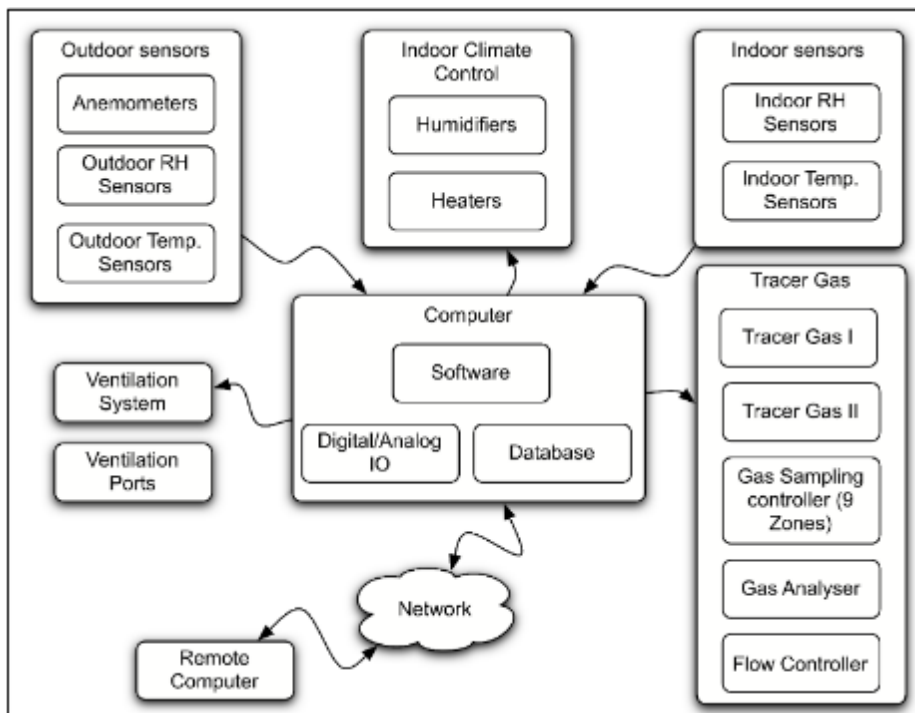
Figure 8. Typical instrumentation scheme using FlexiDAQ.

The injection rate of each tracer gas is controlled by a Red-y Smart controller gas flow meter set via the computer. Flow rates can be adjusted between 0.8–40 mln/min for N_2 and between 1–140 mln/min for carbon dioxide (CO_2).

In addition to the sensors and gas analysers, local weather conditions were recorded using a FLexiDAQ-based weatherstation alongside the ventilation research building. This was located approximately 15 m away and is based on an Agilent 34980 multiplexer, Gill Instruments ultrasonic anemometer and solar radiation sensors.

3.2.5   Insulation performance measurement

The BRANZ heat flux sensor (HFS)[2] was developed by BRANZ in the 1980s as a practical means for enabling field measurements of heat flow in locations such as the walls, ceilings and floors of houses. The uniqueness of the design was the use of two aluminium facings (1.2 mm thickness) as a means of averaging out the heat flow over the relatively large face area of the transducers, thus enabling the measurement to cover an area that included thermal bridges such as framing.

The original design used a 3 mm air gap as an insulation core and a 10-junction thermopile as the sensing element. The primary advantage of the design compared with typical commercially available HFSs is the large size and relatively low cost. The major disadvantages are that the sensors have significant thermal resistance, and the impact it has on heat flow (and thermal resistance) has to be taken into account when calculating results. The significant thickness of the transducers means that generally they have to be used in conjunction with a surround panel with the same thermal resistance to reduce heat flow distortion at the sensor edge. The BRANZ HFSs are best suited for comparative measurements or situations where incremental in situ changes are made to the measurement specimen.

For the current project, the HFS design was modified to improve aspects such as sensitivity, repeatability, ease of calibration and ease of construction. The two 1.2 mm aluminium facings were replaced with 0.7 mm aluminium on one face and an aluminium foil on the other. The original 3 mm air gap core was replaced with 13 mm of closed-cell plastic foam.

The 13 mm core thickness was made up of two layers of 6.5 mm thick foil-faced foam insulation product. This creates a double foil layer in the middle and single foil layers on the outer faces. One of the outer foil layers is then faced with paper (high emittance) to provide one skin of the HFS, and the other foil layer is faced with 0.7 mm aluminium sheet to provide the other skin. The aluminium sheet skin of the HFS goes against the surface of the building element under measurement, and the paper-faced foil skin of the HFS is left facing into the adjacent room. Using the thinner aluminium sheet on one skin and replacing the other aluminium sheet with four layers of foil reduces the thermal mass of the sensor but still achieves the desired effect of spreading out the heat flow over the thermopile array.

The use of the foam core makes the HFSs easier to construct and results in a more reproducible overall sensor thermal resistance and output signal sensitivity than was achievable with the air gap core. The output signal is also boosted both by the thermopile increasing from 10 to 16 junctions and the thermal resistance of the core increasing from 0.1 to 0.36 m^2K/W.

Using the foam material also makes construction of matching surround panels easier than with the air core sensors, as these panels generally do not need to include the 0.7 mm aluminium sheet. The foam core increased the overall thickness of the sensors from 5.4 mm for the air core to approximately 14 mm including thermocouple wire and facings.

---

[2] See *Engineering application of heat flux sensors in buildings – the sensor and its behavior*.

Since the HFS panels have significant thermal resistance, relative to the overall thermal resistance of the floor systems being measured, of between R1.0 and R2.6, the actual heat flow will be less than would occur without the sensor but under the same environment conditions.

By measuring and logging the thermopile output, the system heat flow is determined, and from the associated measurements of interior and exterior temperature, the overall system R-value (including HFS) can be determined. By subtracting off the R-value of the HFS, the system R-value (excluding the HFS) can be calculated and the heat flow estimated for the same environmental temperature conditions but without the heat flow moderating effect of the HFS.

The analysis of the data to determine R-value follows the method outlined in ISO 9869-1:2014 *Thermal insulation – Building elements – In-situ measurement of thermal resistance and thermal transmittance – Part 1: Heat flow meter method*. The 'moving average' method used in ISO 9869-1:2014 calculates the R-value by means of the average of all the instantaneous heat flows and temperature difference data. The average temperature difference across the construction element being measured must be large enough to generate sufficient heat flow and for it to be measured with appropriate accuracy given the sensitivity of the HFS. The data must be recorded and averaged over a sufficient period of time to account for thermal mass effects and to average out noise in the data.

For this project, the HFS panels were used primarily for comparative analysis, i.e. the difference in heat flow (and R-value) associated with changes in average environmental wind velocity and differences in heat flow associated with changes in moisture content in the insulation material. The absolute accuracy of the thermal resistance measurements and the detailed analysis of instantaneous heat flow was of secondary importance. A discussion of in situ heat flow measurement techniques and practical accuracy can be found in Ficco et al. (2015).

Calibration

To best match the spacing of the floor framing of the research building, a sensor size of 600 x 600 mm was chosen. The sensors were installed centred over a single joist, enabling a measurement that includes the effect of any gaps or compression of the insulation where it fits against the framing. That particular sensor size had the added benefit of the being well matched to the 610 x 610 mm plate size of the LaserComp Fox 600 heat flow meter used to calibrate the HFSs.

- 16 type-T thermocouple junctions.
- Type-T thermocouple sensitivity approximately 40 µV/K.
- Thermopile output = 16 x 40 = 640 µV/K.
- Sensor thermal resistance approximately 0.36 m^2K/W.
- Theoretical sensor output 640 x 0.36 = 230 µV/(W/m^2); 1 / 0.230 = 4.35 (W/m^2)/mV.
- Measured heat flow (W/m^2) = 4.35 * sensor output (mV). When measured in the Fox 600 heat flow meter using a range of heat flow from 1 to 100 W/m^2, the signal outputs for a set of 20 HFSs was independent of heat flow and within 10% of the theoretical coefficient.
- Type-T thermocouple sensitivity (µV/K) = 0.0855*T(°C) + 38.61 (for -30 < T < 30).
- @ mean 16°C, sensitivity = 40.0 uV/K with temperature dependence of +0.2%/K.
- Thermal conductivity of foam core approximately 0.038 W/m.K @ 16°C.

- Temperature dependence of conductivity +0.3%/K so R-value sensitivity -0.3%/K.
- Combined effect of thermopile output temperature dependence and foam core thermal resistance gives temperature dependence of HFS output -0.1% /K.
- Since the sensitivity of the data acquisition system is approximately 1 μV, the maximum sensitivity of the heat flow sensor to heat flow is approximately 4 mW.

3.2.6 Sensors and layout

Temperature/moisture

Different sensor layouts were made at different locations, indicated with the Greek letters α, β, γ and δ.

Figure 9 shows how these were configured in a vertical cross-section. The sensor types are indicated by a two-letter code:

- MC = moisture content pins
- TC = thermocouples
- RH = Honeywell RH probes.
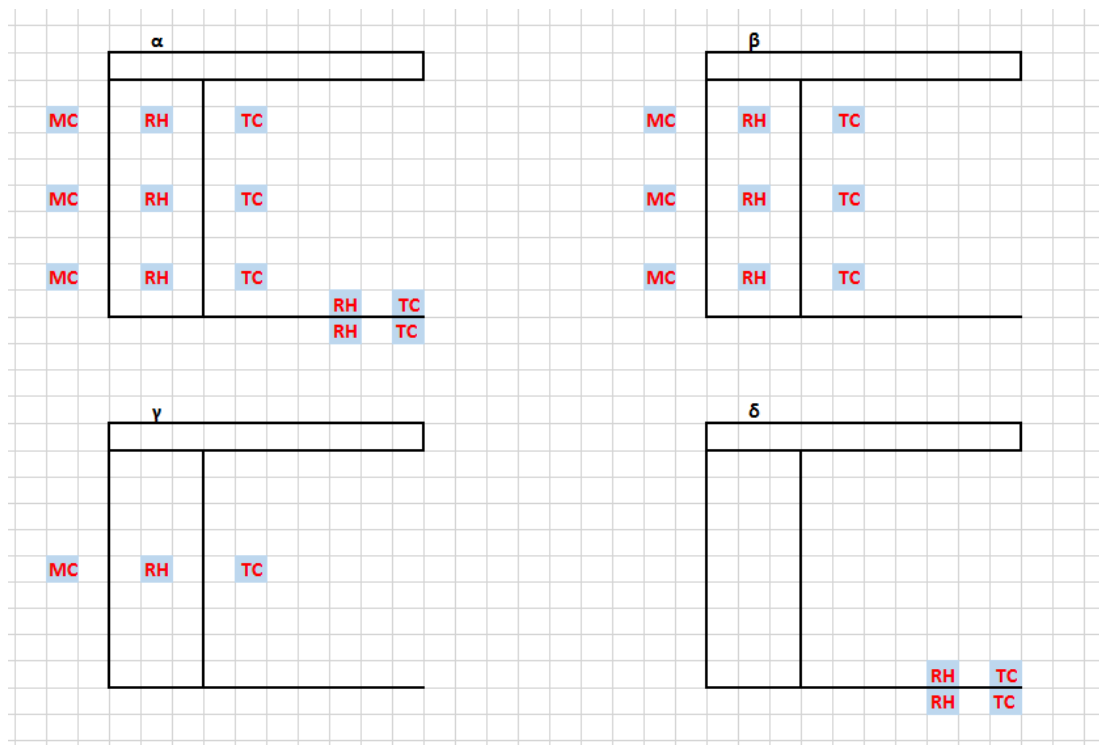
Figure 9. Layout of sensors for each of the four different location types.

Figure 10 shows a plan view of the pile layout under the ventilation research building and the Greek letter associated with the particular sensor layout at each measurement location.
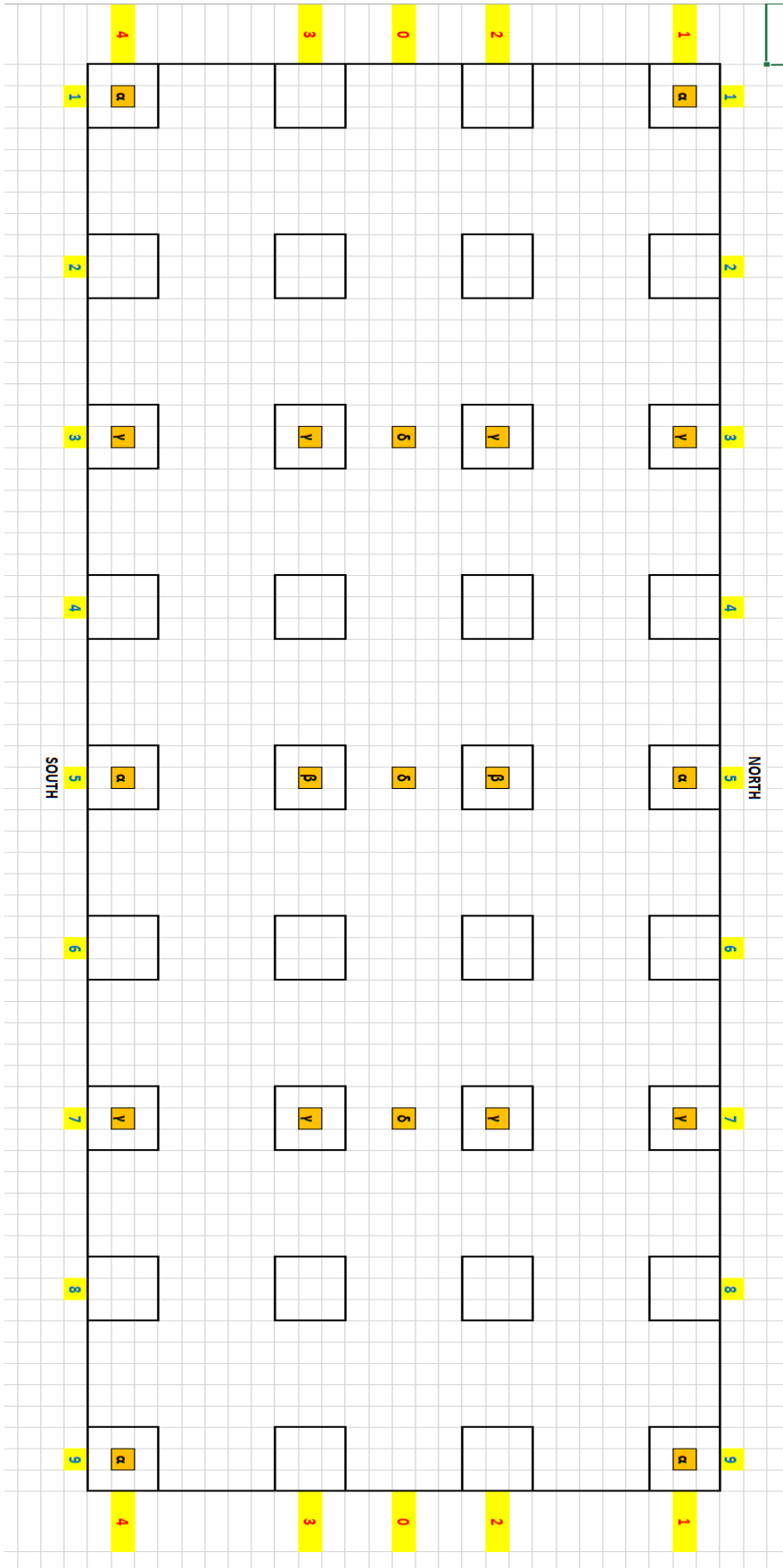
Figure 10. Pile layout and sensor distribution under the ventilation research building.

Moisture content was measured with stainless steel pins set at a standard depth in the timber, and the resistance was measured using a voltage divider with a 1M Ohm resistor and the timber forming the two resistors in the network. 12V was applied to the network for the duration of the measurement, and this voltage was recorded by the Agilent multiplexer. Moisture content was calculated from the voltage measured along with the temperature at that location using the standard formula in Straube, Onysko and Shumacher (2002).

The humidity probes were calibrated using the BRANZ humidifier and were powered with a reference power supply that had a stable output during calibration (as the output of the Honeywell RH sensors depends on the input voltage). During the measurements, a similar supply was used to power the sensors, and the output voltage of this was recorded as a secondary check.

Heat flux sensors

Figure 11 indicates where the heat flux sensors were placed on the floor plan of the ventilation research building.
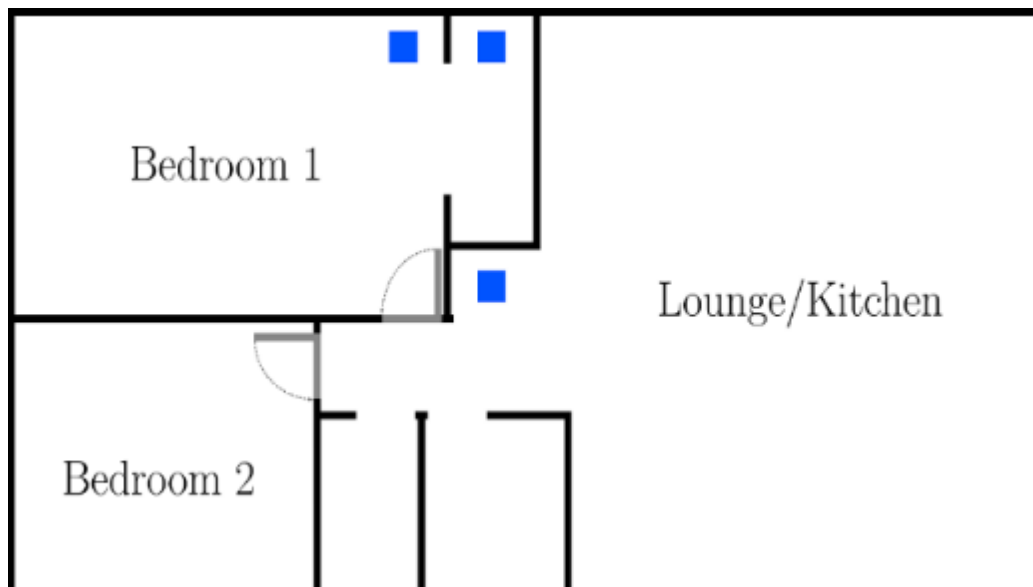
Figure 11. Heat flux sensor locations (shaded blue) in the ventilation research building.

Tracer gas measurement

The subfloor space was equipped with a number of sampling and dosing tubes distributed around the volume. The tubes were typically located 500 mm off ground level. Before the gas monitor analyses the air sample, it purges the tubes and the sampling chamber to avoid cross-contamination. Samples were taken several minutes apart.

The target working concentrations of the tracer gas in the zones is usually at least 10 times the detection limit or, in the case of CO_2, 10 times the background concentration. Tracer gases are sampled from the zones by means of a computer-controlled manifold that can switch each of the possible nine sampling locations onto the gas monitor.

3.3 Insulation performance

3.3.1 Description

The BRANZ fire research building was used to create a second research facility – the subfloor research building (Figure 12) – where the effects of wind wash could be studied more closely without the concern of affecting the ventilation programme measurements taking place in the other lab.

The building is of similar construction to the ventilation research building, with fibre-cement cladding, single-glazed windows and a corrugated steel roof. Where is differs, however, is that the airtightness of the building itself is much lower that the ventilation research building in the order of 10–12 ach @ 50 Pa.

Figure 12. Subfloor research building.

At a height of 1.2 m, the subfloor research building is also considerably higher off the ground compared to the ventilation research building. The subfloor space has been divided in two, with one half closed in with a plywood cladding similar to the other building and the other half been left exposed.

3.3.2 Instrumentation

A FlexiDAQ-based instrumentation system (see 3.2.4) was used to measure a number of heat flux transducers on the floor of the building, and an Ultrasonic anemometer was located underneath the open half of the subfloor.

Figure 13 shows a floor plan of the subfloor research building, with the locations where heat flux sensors were located shaded.
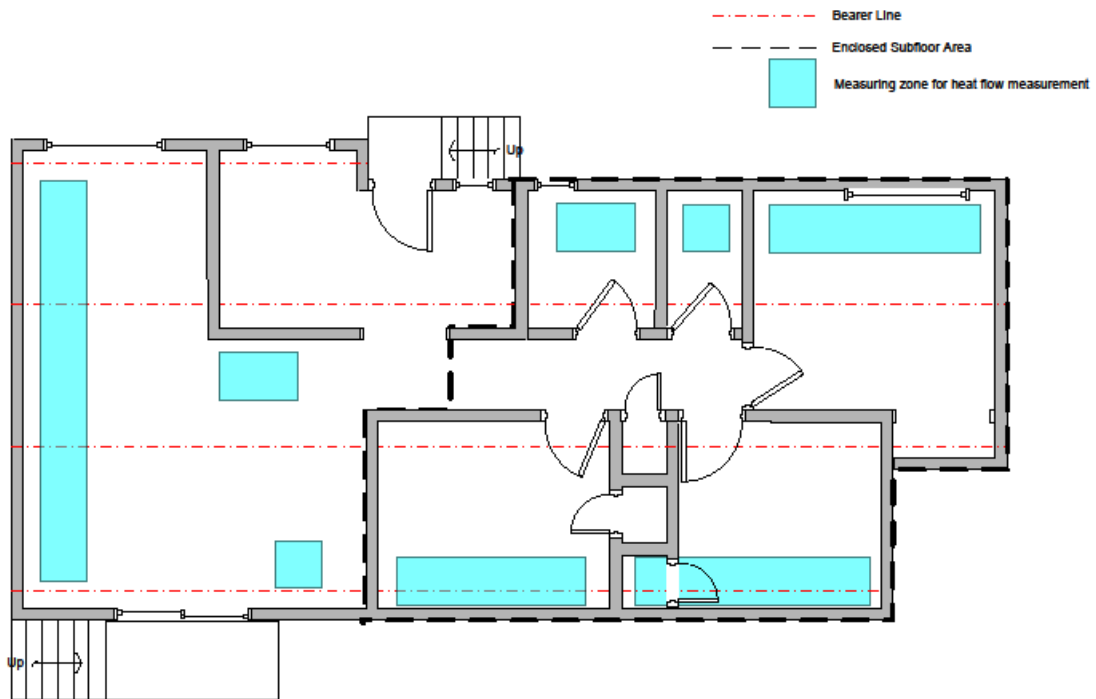
Figure 13. Heat flux sensor locations – subfloor research building.

3.3.3   Indoor conditioning

The conditions inside the subfloor research building were kept relatively constant for the duration where detailed heat flows were calculated using two heat pumps.

4.   Experimental programme

4.1   Field survey results

Results from the field survey are presented below, with section 4.1.1 describing the results of corrosion measurements on the steel plates directly exposed to the subfloor atmosphere. Section 4.1.2 describes the results of the steel sample sandwiched between timber blocks. Section 4.1.3 contains summary statistics of the conditions in the sample houses, including temperature, humidity and moisture content.

4.1.1   Steel directly exposed to subfloor atmosphere

The annual mean corrosion rates of the steel samples exposed to the subfloor environments of the houses surveyed are presented in Figure 14 – Figure 16.
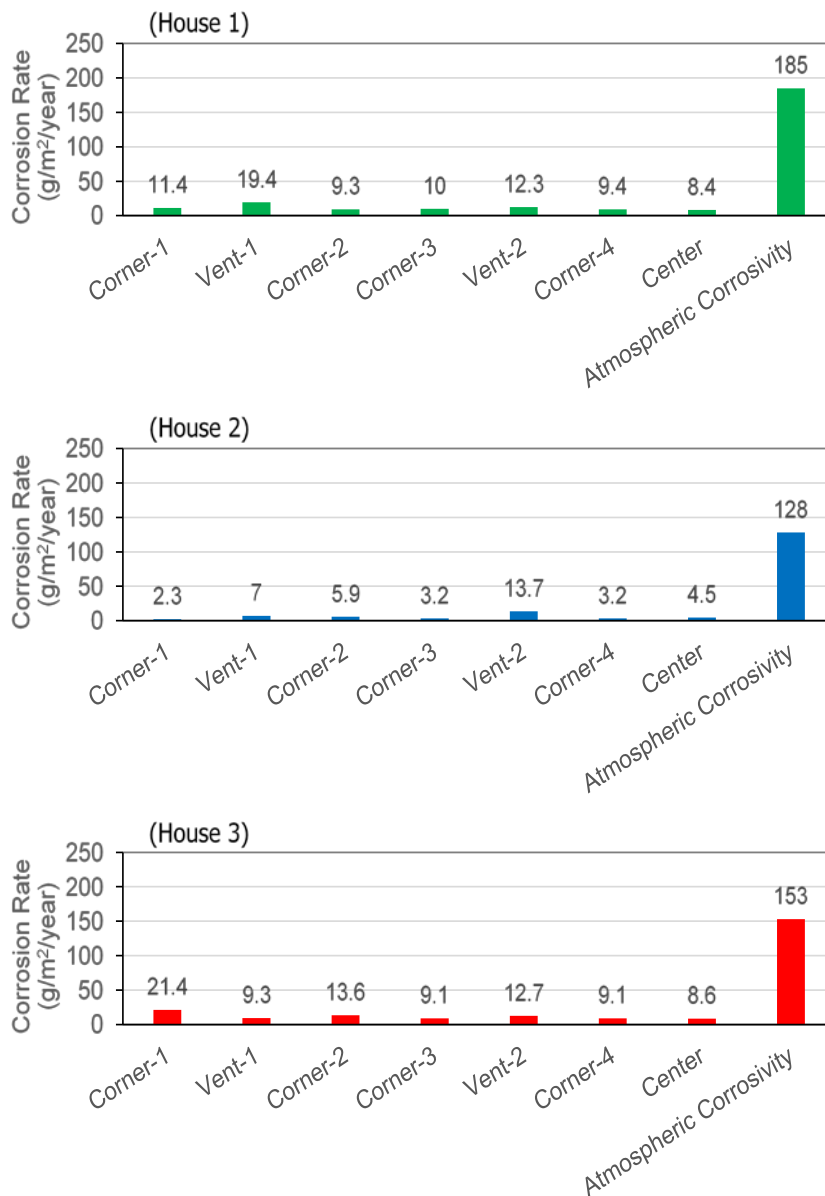
Figure 14. Corrosion rates of mild steel samples directly exposed to subfloor environments of houses surveyed in Auckland.
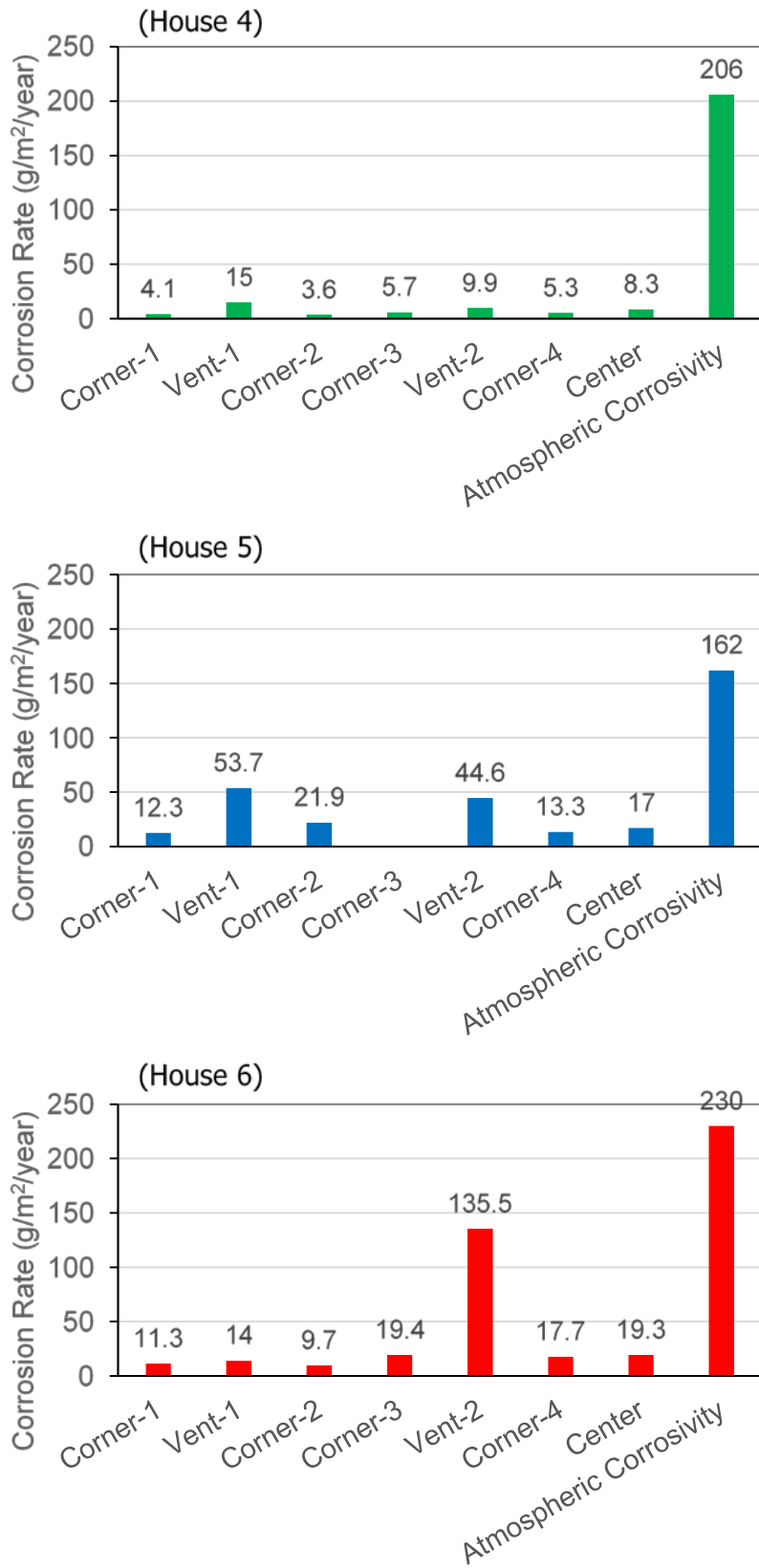
Figure 15. Corrosion rates of mild steel samples directly exposed to subfloor environments of houses surveyed in Wellington.
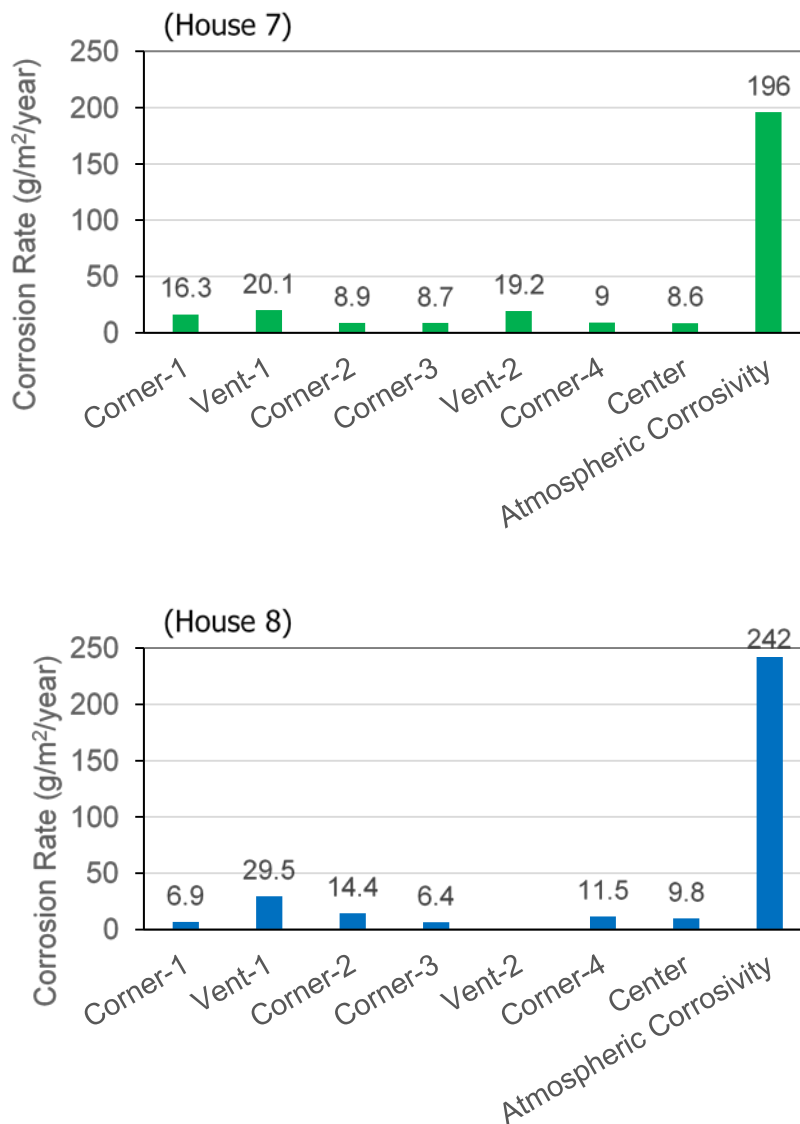
Figure 16. Corrosion rates of mild steel samples directly exposed to subfloor environments of houses surveyed in Invercargill.

It can be seen from these results that the corrosion rates of steel samples installed at corners and the centre of the subfloor were much lower than that of the steel samples directly exposed to the atmosphere surrounding the house surveyed. Typically, the decrease could be 10 times or even more. Although variations could be observed with different corners, these are generally small. There is also no clear evidence that one corner located towards one specific direction would produce a local environment that is more aggressive towards metallic components.

However, these results clearly indicated that metals installed close to subfloor vents tended to corrode more quickly than those situated in corners and the centre. This is particularly true for the subfloors not built with concrete perimeter foundation walls, i.e. those using timber planks. The vent-1 and vent-2 location in house 5 and the vent-2 location in house 6 in particular demonstrate this. Houses 5 and 6 were sitting on concrete foundation corners, and their subfloor enclosures were built using timber planks with gaps (~20 mm wide) between them.

19

Meanwhile, both steel samples installed close to the vent-1 and vent-2 locations in the subfloor of house 5 had similar corrosion rates higher than other locations.

For house 6, it can be clearly seen in Figure 17 that the surface of the mild steel sample close to the vent-2 location was covered with a layer of rust much thicker than that on the sample installed in corners. The difference in corrosion rates between those two samples (corner-2 and vent-2) was 14 times. This phenomenon was not observed with the sample close to the vent-1 location of the same house. This is because the vent-1 location is actually not a vent due to the physical construction. It was only used in this study because it is directly opposite to the vent-2 location.
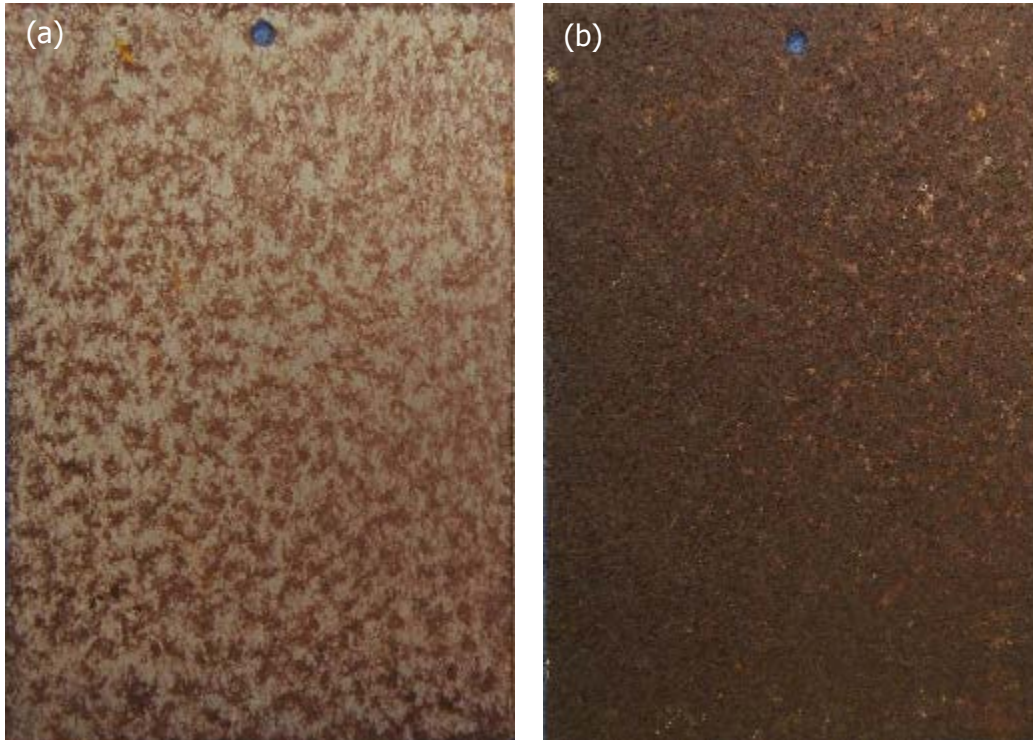
Figure 17. Surface morphologies of mild steel samples installed in corner-2 (a) and close to vent-2 (b) of the subfloor of house 6.

All houses surveyed in this study were not close to the sea and therefore might only be slightly influenced by marine atmosphere, i.e. the effects of sea-sourced salt particles would be extremely limited to metal corrosion within these subfloor environments. As such, the main contributors to corrosion processes would be moisture.

The variations in temperature and relative humidity for corner-2 and vent-2 locations in the subfloor of house 6 are presented in Figure 18. The average values of these two environmental factors were very similar at these two locations. However, the standard deviation of temperature and humidity for the vent-2 location are greater than the corner-2 location. These were 3.1°C and 7.8% RH versus 2.8°C and 5.8% RH for the vent-2 and corner-2 locations respectively. This could lead to higher chance of moisture condensation on the steel surface, i.e. a larger time of wetness, therefore promoting corrosion through a longer period of electrolyte presence. Additionally, the vents on the timber plank subfloor enclosure could also permit ingress of rainwater splash through gaps, resulting in physical water on the steel surface and a longer period of high humidity in the ground nearby and underneath
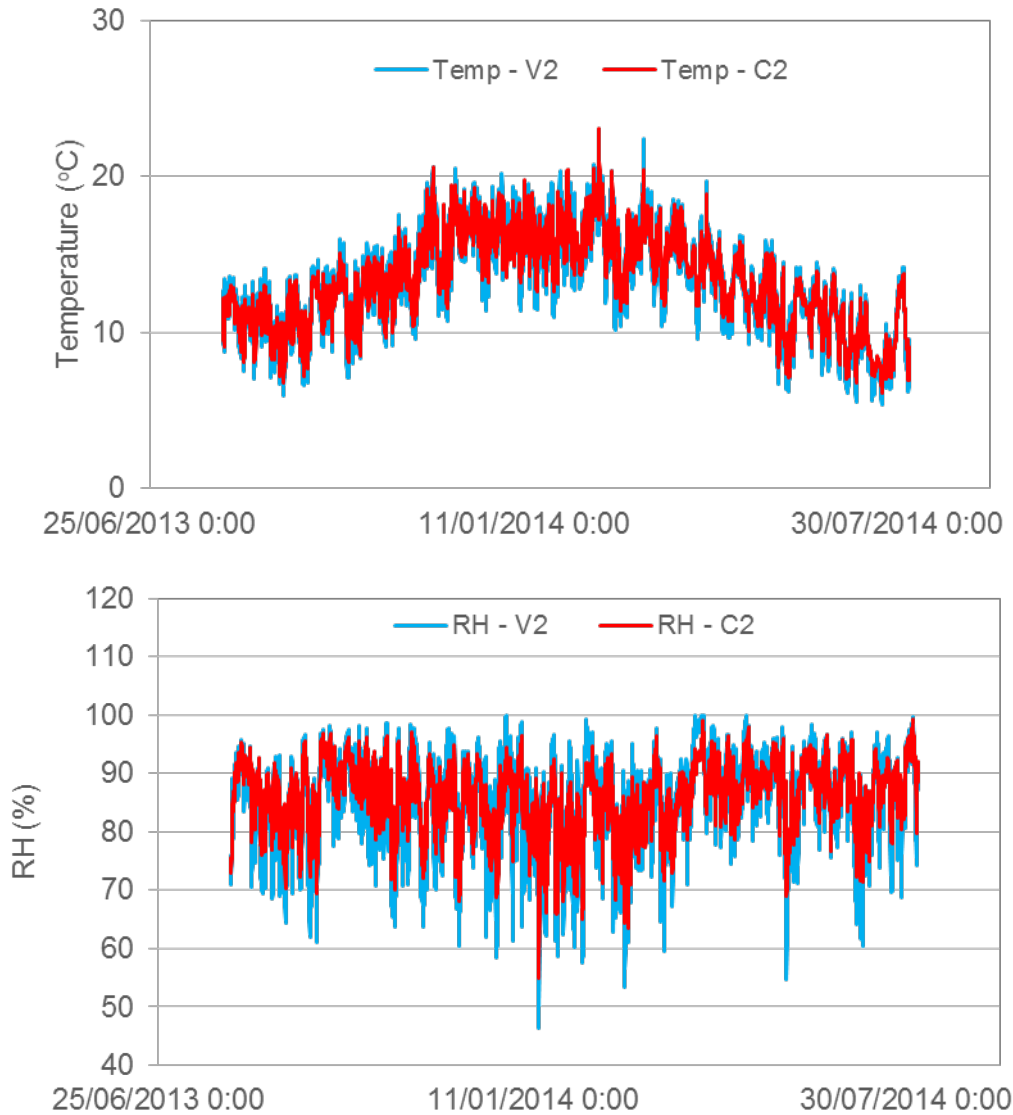
Figure 18. Variations of temperature and relative humidity at corner-2 and vent-2 locations in the subfloor of house 6.

BRANZ's previous studies showed that subfloor ground soils under most New Zealand residential dwellings are rather moist and thus could supply a large amount of moisture to the subfloor spaces, typically >300 g/m²/day. Moisture, if staying in the subfloor environment for long periods, would exert negative influences on metal corrosion through enhanced condensation or increased timber moisture content.

The houses surveyed in this study had a range of different ground conditions. For example, the uncovered subfloor ground of house 5 was very wet all year round, while some uncovered ground appeared to be relatively dry, for example, houses 2 and 6. The ground of most houses was covered with black polyethylene. An attempt was made to investigate how observed ground condition could affect metal corrosion based on corrosion rate measurements in this study. However, due to the small number of houses surveyed, houses with conditions that were highly comparable were not found. Some rough comparisons were then made.

Houses 2 and 3 were built on concrete perimeter foundation walls, and their underfloors were insulated. The ground of house 2 was not covered, and most parts appeared to be relatively dry, while the ground soil of house 3 was very wet but

21

covered (narrow sections along the foundation wall were not completely covered and therefore exposed to subfloor atmosphere). The corrosivity of the surrounding atmosphere of these two houses was also very similar and could be classified as category B according to ISO 9223:2012 *Corrosion of metals and alloys – Corrosivity of atmospheres – Classification, determination and estimation*. The metal corrosion rate measured in the subfloor of house 3 was generally higher than that measured in house 2.

A comparison was then made between the subfloor temperature and relative humidity for houses 2 and 3, mainly for the corner-1 (Figure 19) and centre (Figure 20) locations to explore how this difference happens.
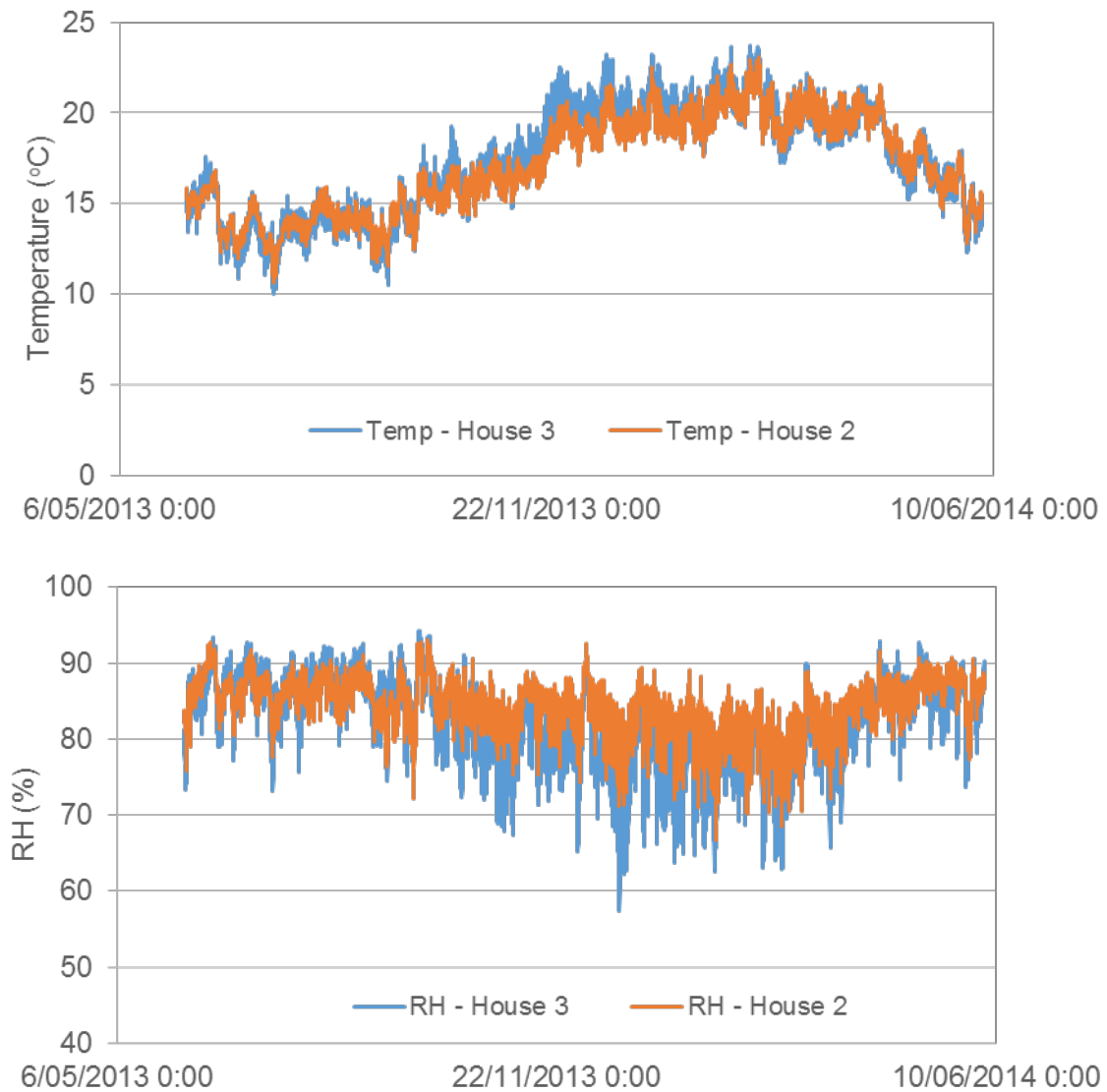
Figure 19. Variations of temperature and relative humidity at corner-1 locations in the subfloors of house 3 and house 2.
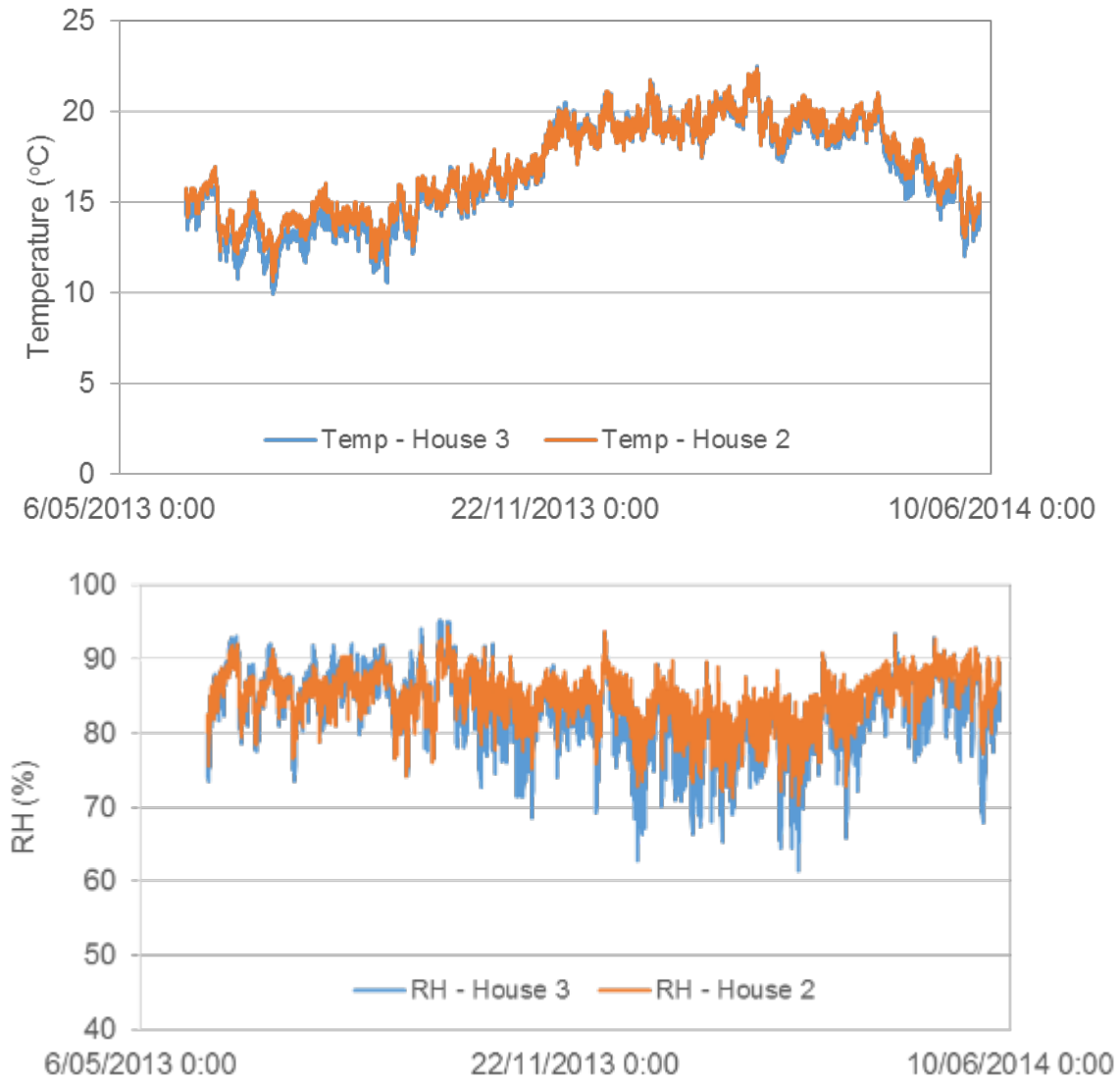
Figure 20. Variations of temperature and relative humidity at centre locations in the subfloors of house 3 and house 2.

Summary statistics from Figure 19 and Figure 20 are presented in Table 1 and Table 2. At the corner-1 locations, in winter, temperature and relative humidity of these two houses were similar although house 3 had a slightly larger variation in RH but only by 1.1%. In summer, house 3 had a higher mean temperature by 0.6°C and a 5.3% lower mean RH.

Table 1. Variation in temperature and relative humidity at corner-1 locations – houses 2 and 3.

	Temperature		Relative humidity	
	Mean	Standard deviation	Mean	Standard deviation
Summer – house 2	19.9	1.1	81.8	3.6
Summer – house 3	20.5	1.1	76.5	5.4
Winter – house 2	14.1	1.1	86.7	2.2
Winter – house 3	13.7	1.3	86.8	3.2

At the centre locations, house 3 had a slightly lower temperature (1.1°C) in winter. In summer, temperatures of these two houses were very similar. However, house 3 had a lower mean RH by 3.7%.

Table 2. Variation in temperature and relative humidity at centre locations – houses 2 and 3.

	Temperature		Relative humidity	
	Mean	**Standard deviation**	**Mean**	**Standard deviation**
Summer – house 2	19.6	0.9	82.1	3.6
Summer – house 3	19.6	0.9	78.4	5.1
Winter – house 2	14.2	1.1	86.1	2.4
Winter – house 3	13.3	1.1	86.1	3.4

In addition, during winter, the corner-1 location of house 3 had a higher humidity than the centre location (86.8% versus 86.1%).

Metal corrosion rates measured at the corner-1 and centre locations of house 3 were nine and two times higher than those measured at house 2, respectively. However, it should be noted that metal corrosion rates measured at these two locations of these two houses were relatively small.

Considering the temperature and humidity values and their variations observed within these two subfloors, it appears that the location with wet, uncovered, ground soil would show larger temperature and humidity variations, especially during winter. This could promote condensation on metal surfaces, possibly for longer periods, therefore enhancing corrosion.

Meanwhile, ground coverage could decrease local environmental humidity by inhibiting direct moisture evaporation from wet ground soil, exhibiting positive effects on metal corrosion performance (for example, the corner-1 versus centre locations of house 2).

In comparison, the ground soil conditions of houses 5 and 6 in Wellington were quite different. House 5 was very wet, with water ponding on some parts, particularly during winter, while house 6 was reasonably dry.

Metal corrosion rates measured at corner and centre locations of these two houses were quite similar although higher rates would generally be expected with house 5 due to its much wetter ground, which could produce more moisture.

It is noticed that these two houses were using long timber planks for construction of the subfloor enclosure. Gaps between planks ~20 mm wide could provide natural ventilation to these subfloors, which might be sufficient to provide enough air exchange to remove moisture effectively. During BRANZ's field visits, timber joists showing signs of high moisture content were not observed.

As shown in Figure 21, both temperature and relative humidity in the centre locations of these two houses were exhibiting no significant difference. This could then explain why metals tended to corrode similarly in these two subfloors with significantly different ground soil conditions.
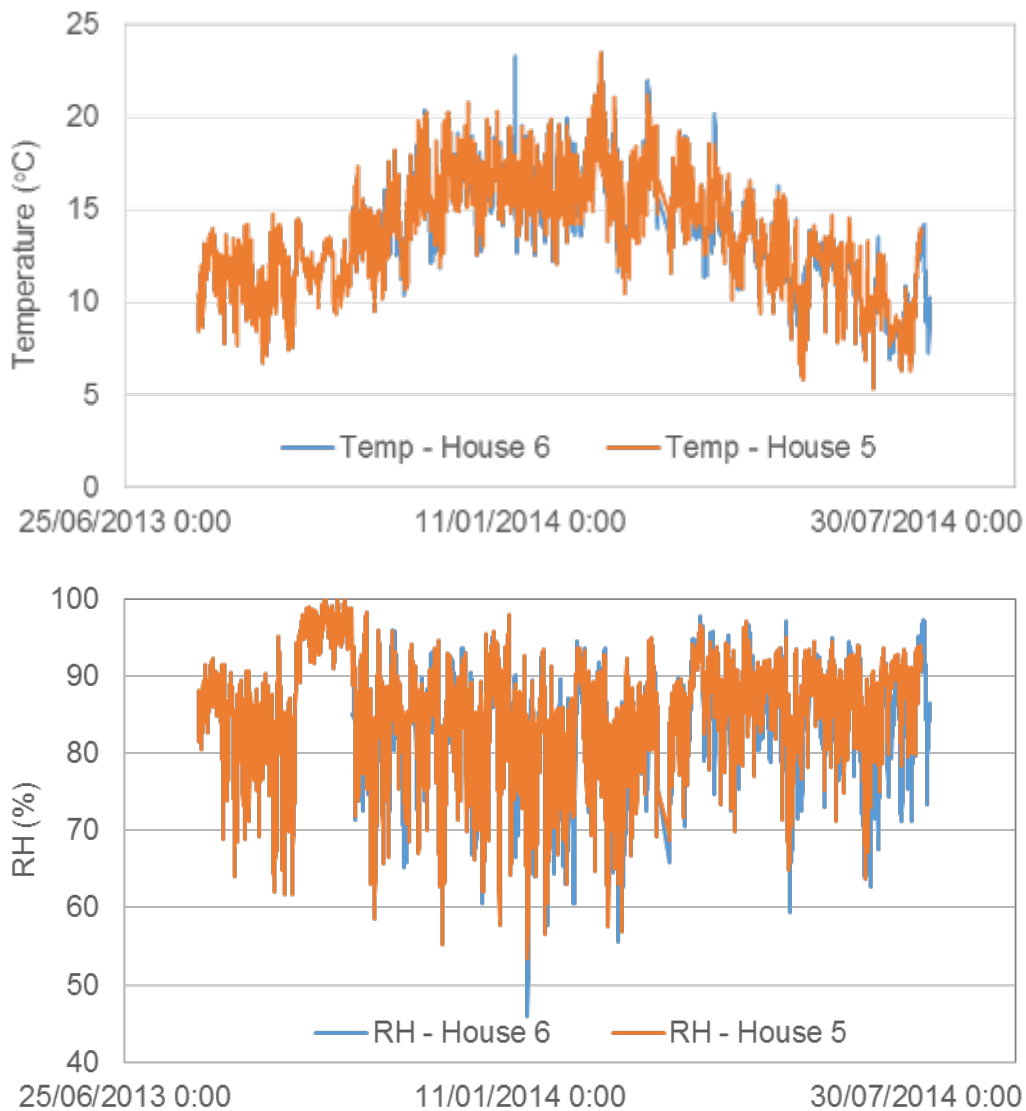
Figure 21. Variations of temperature and relative humidity at centre locations in the subfloors of houses 6 and 5.

4.1.2   Steel sandwiched between timber blocks

The annual mean corrosion rates of the steel samples sandwiched between H3.2 CCA-treated timber blocks that were exposed to the subfloor environments of the eight houses surveyed are presented in Table 3.

In comparison with the metals directly exposed to subfloor atmospheres, these samples corroded even slower. Only limited patches with very thin rust could be observed after 12 months of exposure (Figure 22).

Most of the corrosion rates were very small and therefore no clear trends regarding location, ground condition or ventilation could be derived with high confidence. However, this might be implying that moisture contents in timbers exposed to these subfloor environments were low, possibly lower than the threshold for fast corrosion (i.e. 20–22%) in most periods.

Table 3. Corrosion rates of mild steel samples sandwiched into H3.2 CCA-treated timber blocks (g/m²/year).

House	Corner-1	Corner-2	Corner-3	Corner-4	Vent-1	Vent-2	Centre	Atmosphere
House 1, Auckland	2.1	1.5	3.1	3.0	2.4	1.4	2.0	185 (B)
House 2, Auckland	1.2	11.3	3.1	2.2	1.5	1.7	1.5	128 (B)
House 3, Auckland	2.3	8.0	5.0	4.3	1.2	6.2	2.3	153 (B)
House 4, Wellington	0.4	0.8	4.4	0.7	1.5	1.7	0.1	206 (C)
House 5, Wellington	1.8	2.8	-	1.5	3.6	5.0	2.4	162 (B)
House 6, Wellington	3.4	2.3	4.9	2.0	1.8	7.1	1.0	230 (C)
House 7, Invercargill	12.5	1.3	19.6	5.5	93.2*	8.6	1.0	196 (B)
House 8, Invercargill	2.6	3.0	8.9	2.2	5.3	-	2.8	(C)

* Timber wetted by rainwater through vent.

Exposed	Sandwiched		Exposed	Sandwiched
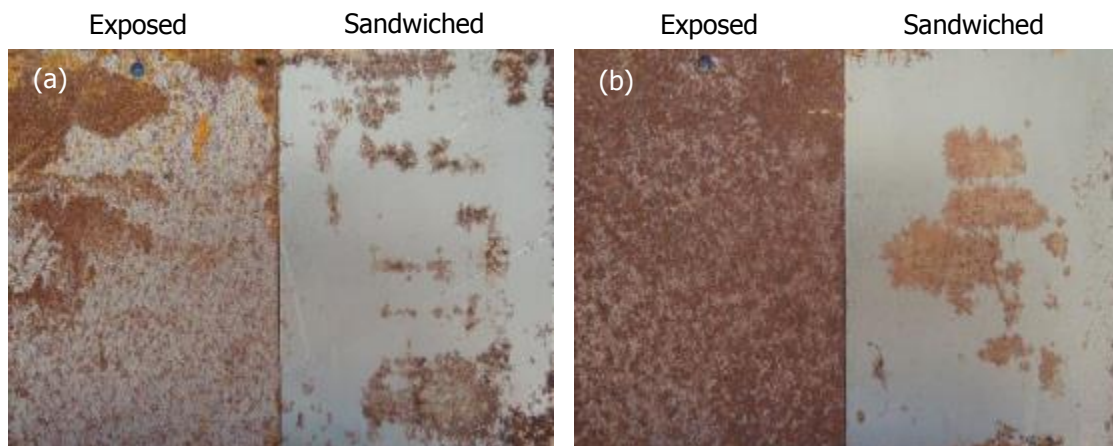
Figure 22. Surface morphology of mild steel samples exposed to subfloor of house 7 (a) in the corner of the house, (b) close to vent 2.

From Figure 22(a) and (b), it appears that the sample close to the vent suffered slightly more corrosive attack than that installed in the corner. The chance of moisture condensation on the steel surface could be higher due to larger variations of temperature and humidity close to the subfloor vent.

The sample sandwiched into the timber blocks installed at the vent-1 location of the subfloor of house 7 had a high corrosion rate, 93.2g/m²/year. An examination of the steel surface and timber revealed that this sample had been wetted by water for a relatively long period (see Figure 23). A check of the foundation wall arrangement showed that the external concrete pavement close to this vent was high. Consequently, rainwater could flow into the subfloor through this vent and make the timber block wet.

Figure 23. Surface morphology of sandwiched mild steel sample installed close to the vent-1 location in the subfloor of house 7.

4.1.3   Summary statistics

Table 4 to Table 6 summarise conditions in each of the survey homes for temperature, timber moisture content by mass and relative humidity.

Table 4. Mean annual temperature for each house.

	Mean (°C)	Min (°C)	Max (°C)	Sd (°C)
House 1	16.8	8.8	23.3	2.9
House 2	17.0	10.7	22.4	2.5
House 3	16.6	9.9	22.5	2.8
House 4	15.7	9.6	26.2	2.3
House 5	14.1	5.8	23.5	2.7
House 6	14.1	6.4	22.7	2.8
House 7	13.2	3.9	17.8	1.7
House 8	11.5	3.9	18.0	2.6

Table 5. Mean annual timber moisture content for each house.

	Mean (%)	Min (%)	Max (%)	Sd (%)
House 1	9.2	5.3	10.5	0.7
House 2	12.5	10.2	15.0	1.0
House 3	12.3	2.7	15.5	1.6
House 4	11.6	2.3	13.2	0.6
House 5	8.7	6.7	13.5	0.9
House 6	14.5	5.5	23.2	1.8
House 7	13.6	5.8	18.8	1.2
House 8	6.8	2.2	9.3	1.6

Table 6. Mean annual relative humidity for each house.

	Mean (%)	Min (%)	Max (%)	Sd (%)
House 1	74.3	51.0	90.0	6.4
House 2	84.8	70.3	94.3	3.5
House 3	82.5	61.5	95.3	5.4
House 4	77.9	54.8	89.6	5.6
House 5	85.1	53.4	100	7.2
House 6	83.1	46.0	97.7	7.1
House 7	86.6	54.9	96.4	3.4
House 8	86.2	56.1	95.0	4.2

4.2 Ventilation research building

The main thrust of the experiments undertaken under the ventilation research building were designed to understand the processes that take place with respect to subfloor moisture and determine the optimum strategy to manage this moisture. This can take the form of limiting evaporation with ground cover and optimising ventilation strategies while also considering the effects of subfloor moisture on fastener corrosion and insulation performance.

In order to understand the movement of moisture in the space, standard measurement techniques were employed. These include measuring the conditions in the space in multiple locations (temperature and RH) and measuring moisture content of timber specimens in the space. From there, a set of experiments were carried out to get a picture of the effect of different parameters on the subfloor.

The remaining piece in the puzzle is understanding the air movement. In doing this, a set of tracer experiments were completed in conjunction with modelling using CONTAM to generalise these.

4.2.1 Experimental timetable

A timeline of the experimental work is given in Table 7. Further descriptions of each phase and the results are given in the remainder of this section.

Table 7. Ventilation research building experimental timetable.

Phase	Start date	Notes
Conditioning	January 2013	Subfloor enclosed, but main doors left open. Instrumentation came online towards the end of this phase.
Accumulation	December 2013	Doors and all vents closed, concentration decay experiment completed during this time.
Ventilation added (20% of Building Code)	May 2014	Set of 10 90 mm vents added, concentration decay experiments completed during this time.
Additional ventilation	December 2014	90 mm diameter vents exchanged for 200 mm.
Closure and addition of polythene	June 2015	All vents closed and polythene ground cover added, longer-term constant emission gas tracer experiment completed.

4.2.2 Conditioning

The ventilation research building was relocated to the BRANZ site in Judgeford in 2010. The subfloor space to this building remained completely exposed to the environment until the beginning of the subfloor research programme. In early 2013, a plywood cladding in combination with a sand and polythene-based footing (Figure 24) were added to enclose the space. Large doors were fitted at either end of the building to enable access.
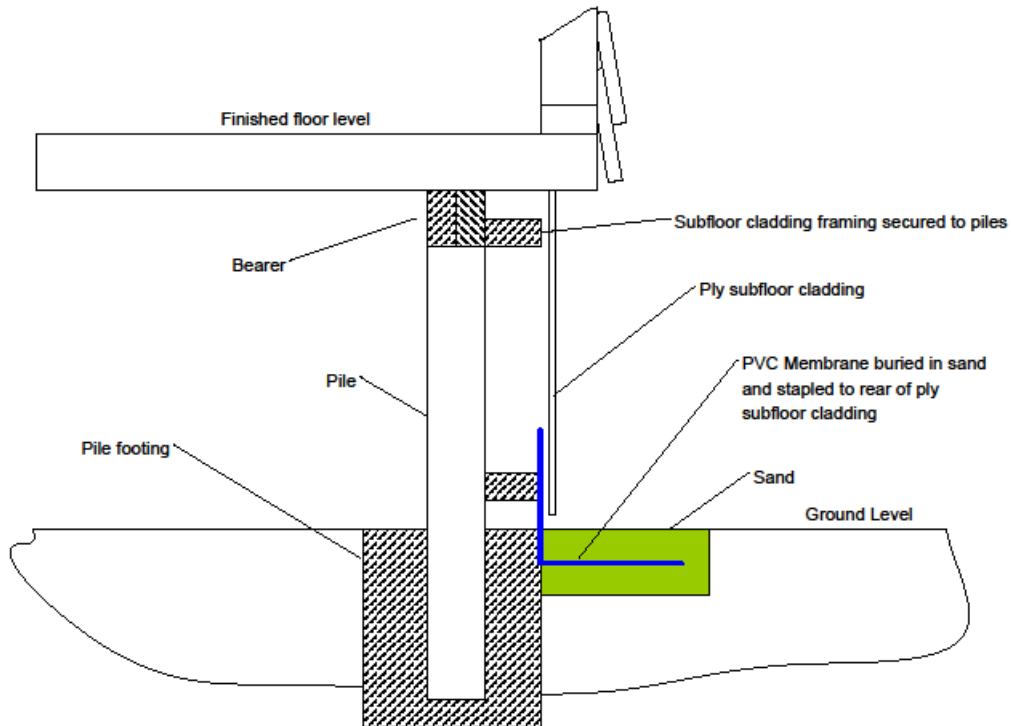

Figure 24. Subfloor footing detail.

Prior to closing the door, the instrumentation was turned on and state of the subfloor captured. This is shown in Figure 25 via a heatmap of timber moisture content of the subfloor framing timber. This floor plan is rotated 90 degrees relative to Figure 10.
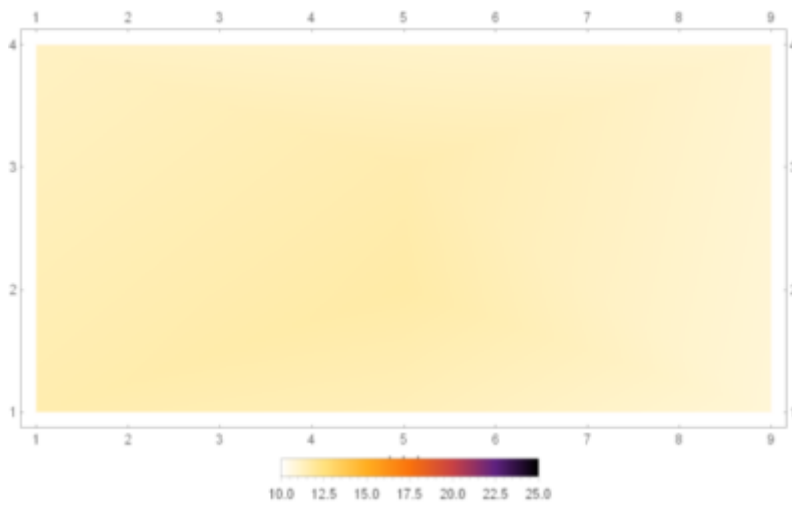

Figure 25. Heatmap of timber moisture content prior to enclosing the space.

29

Figure 26 is a plot of the mean timber moisture content prior to the doors being closed. The timber was in a consistently dry state around 12% across the entire space.
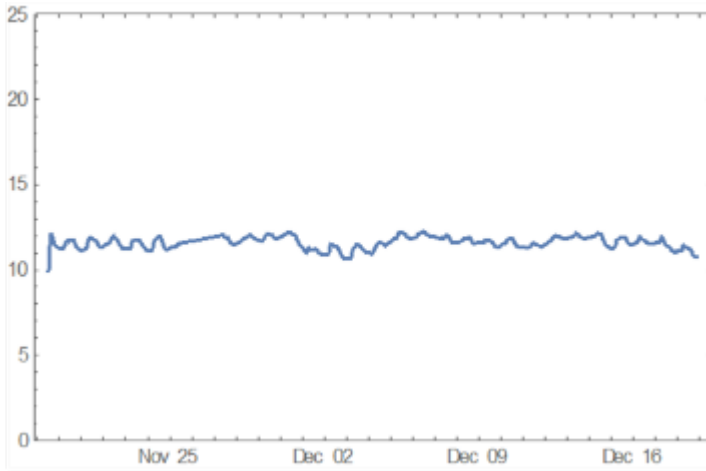

Figure 26. Mean moisture content for the 3 weeks prior to enclosing the space.

4.2.3 Accumulation

In late December 2013, the large doors at the ends of the building were closed and sealed shut. The ground was uncovered (there was no polythene in this configuration). From this point, the conditions in the space were monitored closely.

Figure 27 is a plot of the moisture content in a timber bearer along the south face of the building. Figure 28(a) shows a heatmap of timber moisture content just prior to additional ventilation being added. It is clear that the southern side of the subfloor space has accumulated considerably more moisture, mainly due to the lack of solar gain on the plywood lining of the subfloor and the floor surfaces of the rooms above.
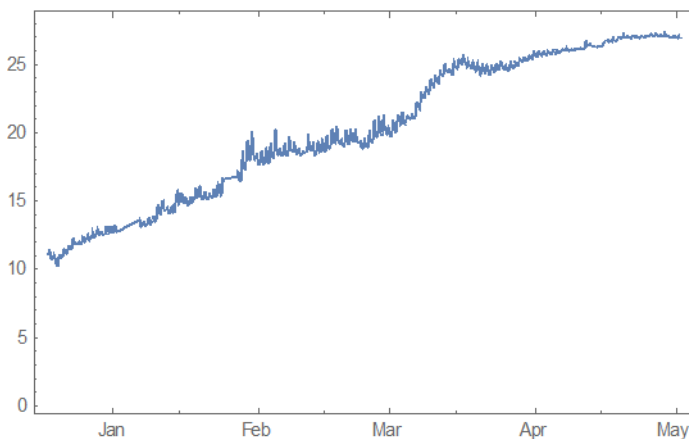
Figure 27. Moisture accumulation in southern subfloor framing timber.

As Figure 27 shows, the accumulation of moisture in the framing once the doors were closed is rapid, taking 4 months to build up from a dry state to reach fibre saturation, purely from absorption from moisture in the air. Using the equipment mentioned in section 3.2.3, the leakage area of the entire subfloor space to outside was measured to be roughly equivalent to a single pipe of 150 mm diameter. Figure 27 and Figure 28 clearly show that the amount of infiltration this provides is insufficient to dilute the moisture evaporating from the exposed soil in the space.

4.2.4   Ventilation added

In May 2014, the steel plates covering the vents in the subfloor walls were exchanged for a set of vents at 90 mm diameter. These were chosen as they represented what had been found was in use in practice over numerous BRANZ houses condition surveys and the field survey. The drying of moisture after this occurred can be seen in Figure 29. Figure 28(b) shows a heatmap of the subfloor framing timber in December of 2014, where it is clear the subfloor space has recovered to a large extent, with a mean of 13.5%.
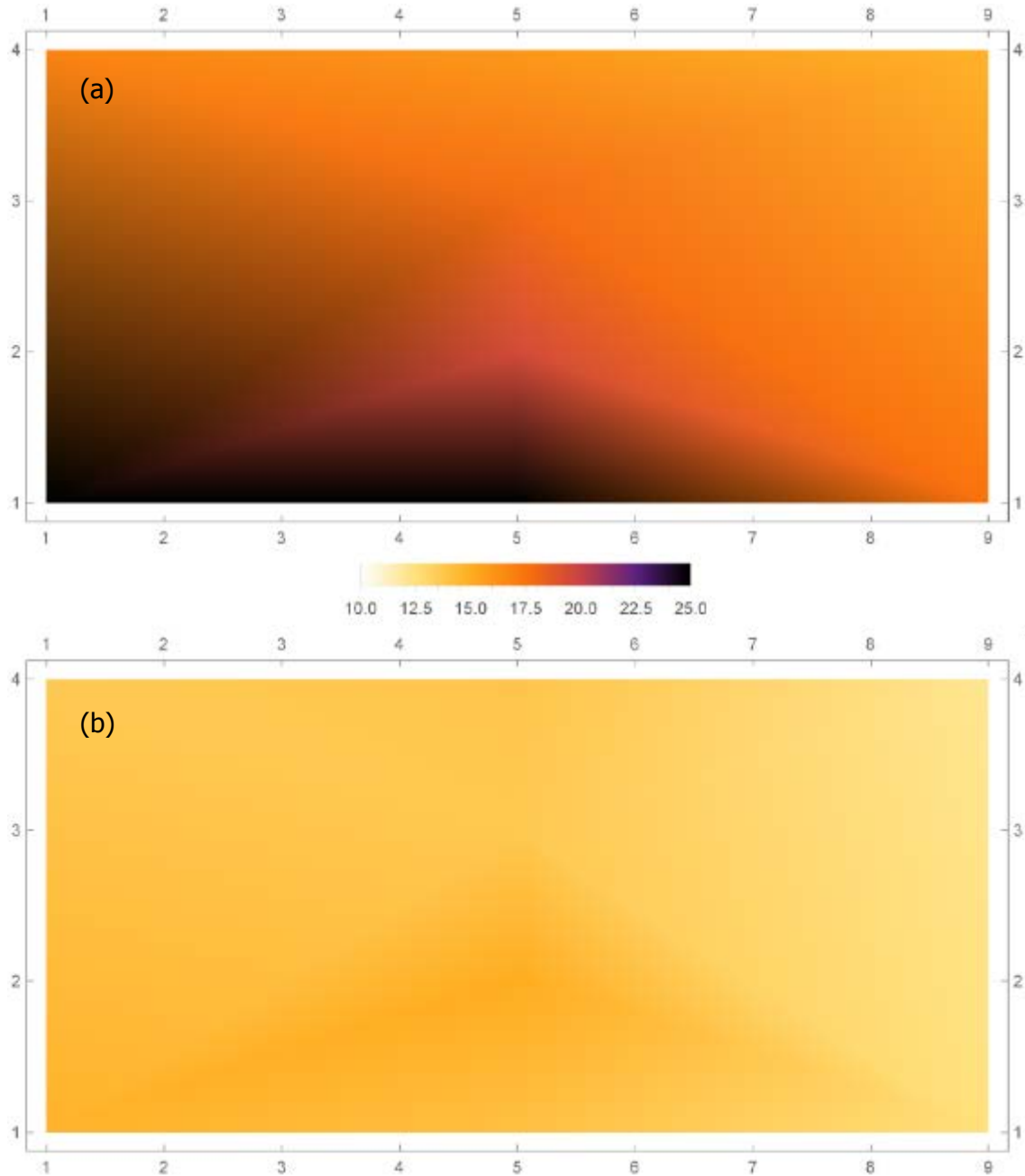
Figure 28. Heatmaps of framing moisture content – (a) in May 2014 and (b) in December 2014, some time after vents were added.
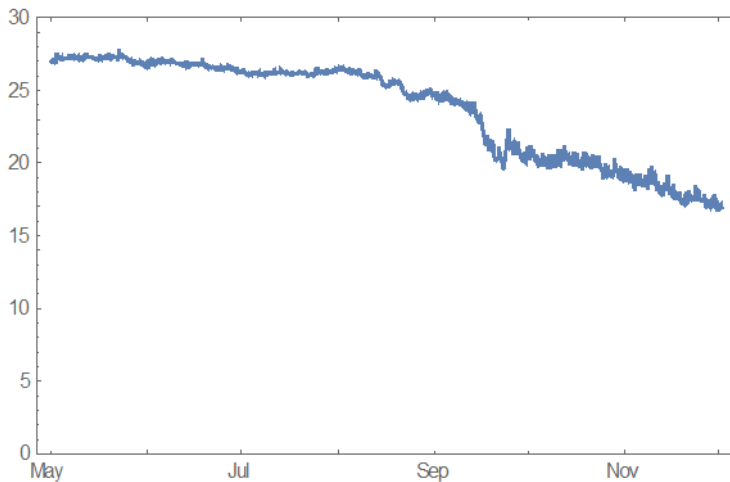
Figure 29. Drying of framing timber after the addition of 20% of Building Code level ventilation openings.

Figure 28 and Figure 29 clearly demonstrate that the addition of ventilation openings is beneficial to the amount of moisture retained in the subfloor. The remaining question is how much ventilation those vents provided. Given that this building is in a well exposed location, we cannot be sure that similar openings will be sufficient in built up areas or where site conditions of other works may limit the effectiveness of the vents provided.

4.2.5 Additional ventilation

In December 2014, the smaller 90 mm vents were replaced by a set of 200 mm diameter vents. There was little difference to the moisture in the timber noticed at this point, as the subfloor has already dried from the earlier accumulation. The larger vents may have enhanced the speed of drying. However, due to the time investment required to get moisture to accumulate for a second time, it was deemed not necessary. The ventilation rate provided by the larger vents was able to be calculated using CONTAM and the tracer experiments in the following section.

4.2.6 Gas tracer experiments

Two forms of tracer gas experiments were completed to measure ventilation rates in the subfloor – these consisted of tracer decay and constant dosing experiments. Tracer decay measurements were made after fitting the first set of vents to the building and when the second 200 mm set were added. These experiments dosed a pulse of N_2O into the subfloor, and the concentration was measured as it was diluted by the ventilation process – the concentration decay gives a time constant correlated to the ventilation rate. This calculated rate is only valid for the period of the measurement though, as wind speed and direction and temperature will change this result with time.

Results are plotted in Figure 30 and Figure 31. Ventilation rates for the 90 mm and 200 mm vents were 25.9 and 32.6 ach respectively.
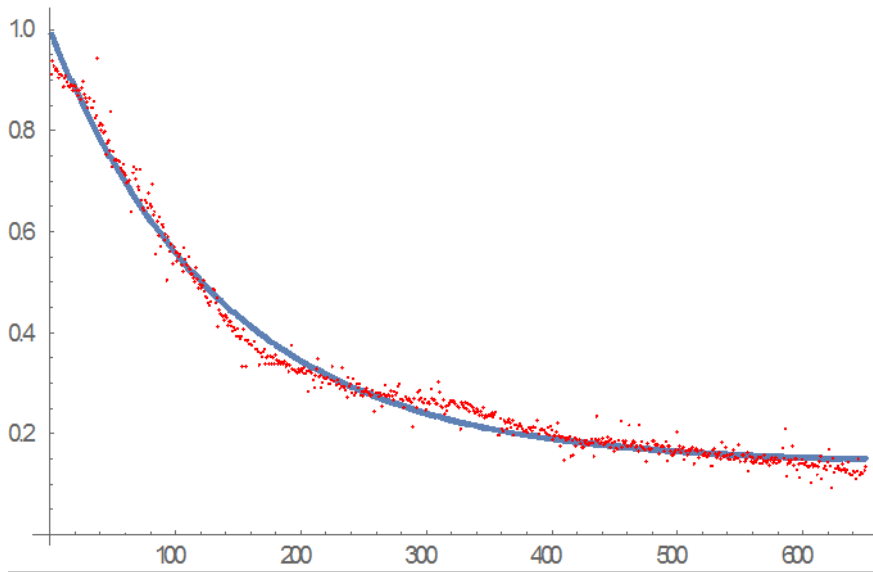
Figure 30. Tracer decay – 90 mm vents.
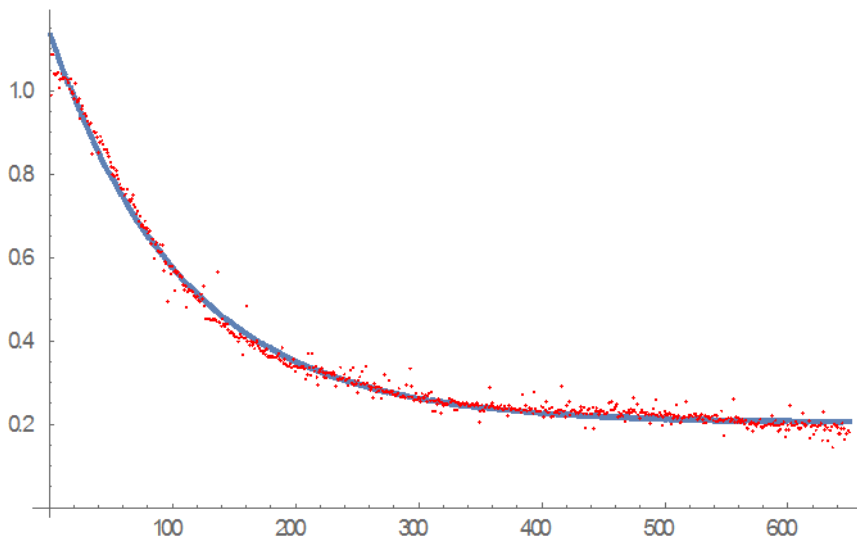
Figure 31. Tracer decay – 200 mm vents.

Since a decay measurement has a limited usefulness and consumes a large amount of N_2O, the tracer gas was changed to SF_6 and the Lumasense analyser was to perform a constant dosing experiment. The wide dynamic range of the Lumasense analyser meant that it could be used to measure subfloor air exchange rates for a relatively long period. It was deployed in September 2015 for about a month while the subfloor was fully sealed and polythene was laid on the ground. This gave a picture of the variability of the infiltration/ventilation.

Hourly average ventilation rates are plotted for the measurement period in Figure 32. The mean measured ventilation rate was 11.5 ach.
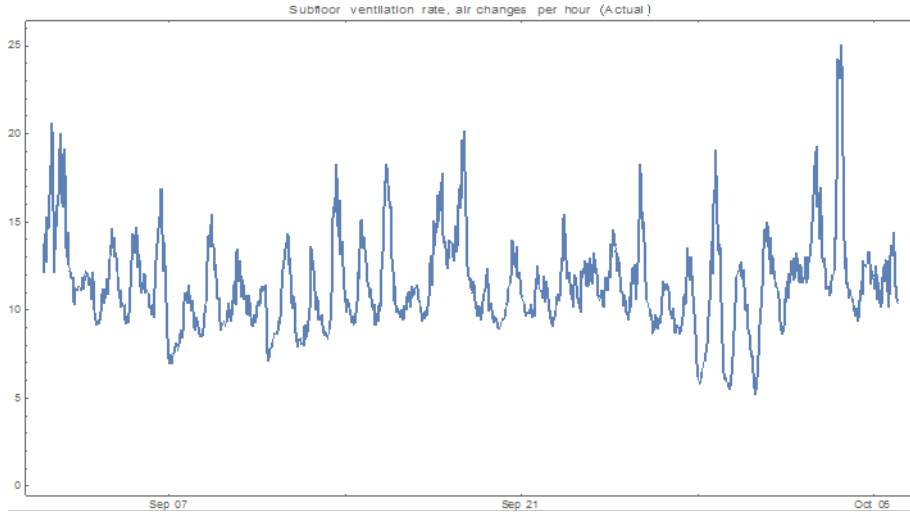
Figure 32. Hourly average ventilation rates measured in the subfloor – all vents closed and polythene laid on the soil.

Figure 33 and Figure 34 are plots of the hourly average wind speed (measured at a height of 10 m) for the period of the measurements shown in Figure 32 and the rest of the project respectively. The mean in Figure 33 was 2.27 m/s, and in Figure 34, this was 2.11 m/s.
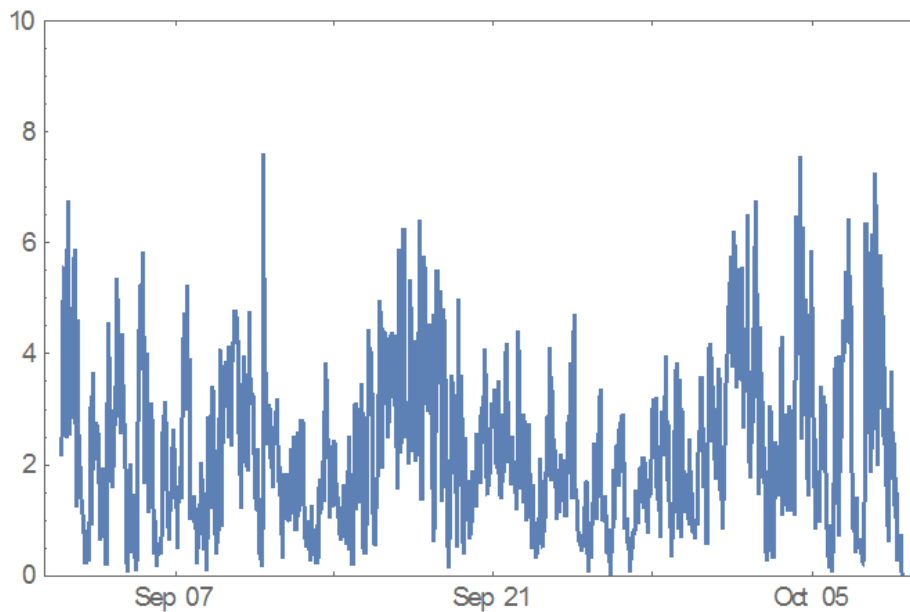
Figure 33. Hourly mean wind speed during constant dosing tracer experiment.

The range wind speed is fairly similar in both plots, and the mean speeds are close enough to give confidence that the infiltration rates in Figure 32 are typical for the enclosed subfloor with no ventilation provisions.
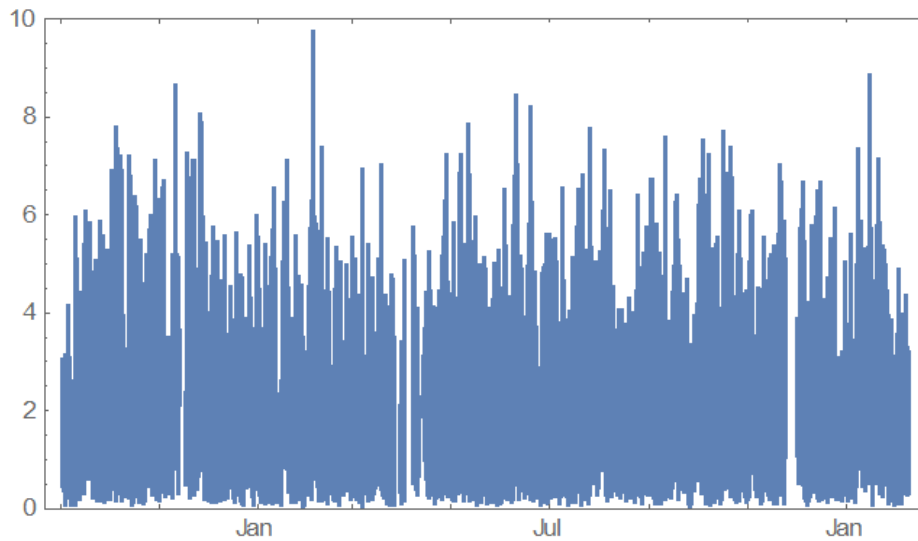
Figure 34. Hourly mean wind speed over the project.

This also gives confidence that the ventilation rate during the accumulation experiment (where the Lumasense analyser was unavailable) was similar and that a mean rate of 11.5 ach is valid for use in WUFI models of the subfloor space.

4.2.7 Ground covering

As seen in Table 7, the subfloor was sealed again in June 2015, and a polythene moisture barrier was laid on the ground. The moisture content of the bearer on the south face (where the highest moisture contents were previously measured) is shown in Figure 35.
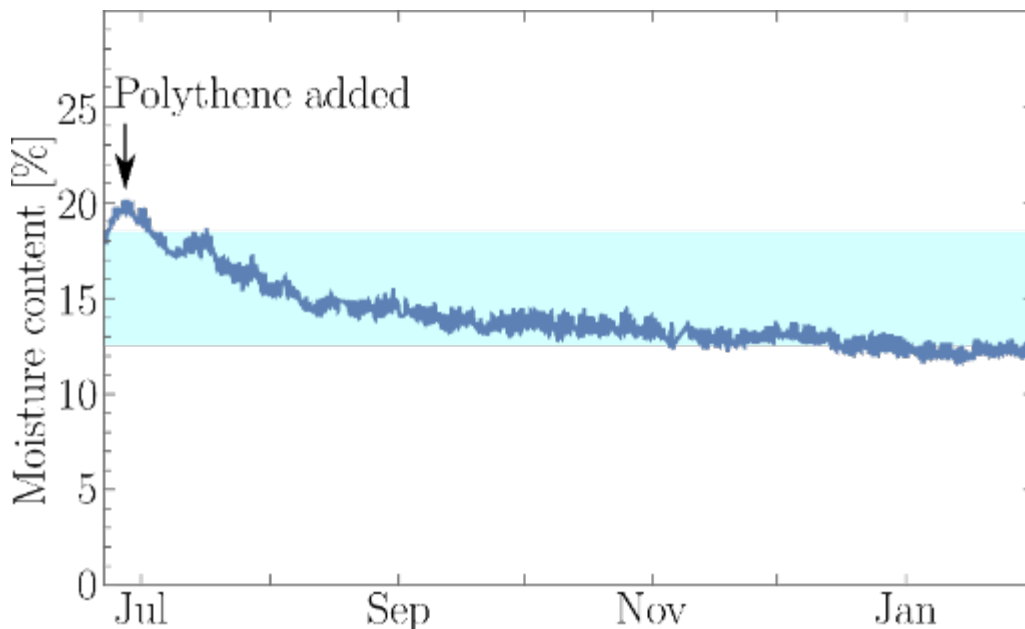
Figure 35. Moisture content of south bearer after polythene laid and all vents of the space are closed.

4.3 Insulation performance

4.3.1 Monitoring the performance of draped foil

The purpose of these measurements was to determine the impact that wind wash has on draped foil. Although the (older) subfloor research building had existing 30-year-old draped foil floor insulation, as a result of the building being used previously for fire testing, the foil was found to be in such poor condition that it was unsuitable for testing. Since draped foil is known to lose some of its reflectivity and therefore thermal performance with age, the results of measurements on relatively new foil to establish the initial or best performance possible are preferred.

The ventilation research building was also built with draped foil insulation, however, the foil was effectively new. Before the foil was replaced with bulk insulation, the thermal performance was monitored for a 2-week period at the end of May 2012. Since the subfloor area was not enclosed until May of the following year, the foil insulation was exposed to direct wind wash. The floor joists of the ventilation research building are aligned in a north-south direction, and so before enclosure of the subfloor area, the insulation was significantly exposed to the prevailing northerly winds.

Heat flux sensors were installed on the top surface of the bare flooring at three locations – one near the south-facing wall, one near the centre of the floor and one near the north-facing wall (Figure 11). Further details of the technique can be found in BRANZ Study Report SR202 (Cox-Smith, 2008), which describes measurements of the thermal performance of draped foil floor insulation using an earlier version of the BRANZ heat flow sensors.

The technique used in SR202 was based on the use of a heating box to generate a significant temperature difference between the floor surface and the subfloor airspace. The heating box was not required in this work, as the ventilation research building indoor environment was under a controlled heating regime as part of the WAVE project. SR202 includes a detailed description of the method for calculating thermal resistance from the heat flow and temperature measurements, calibration of the HFSs, and a discussion of the uncertainties involved with the measurements. (A description of the HFSs used for the current project is given in section 3.2.5 of this report.)

The wind conditions used in the following analysis were measured at 10 m above ground. Later measurements of wind conditions in the subfloor space before it was enclosed determined the direction to be the same but the velocity to be approximately one-tenth of the velocity at 10 m (see section 4.3.2).

Figure 36 shows a summary of the wind speed and direction over the measurement period. The data has been summarised as a 24-hour moving average of wind speed and direction with the direction split into two components – north to south and east to west. Data points are at 1-hour intervals. It can be seen from the chart that strong northerly winds were experienced on 27 and 28 May, moderate southerlies on 20 May and moderate easterlies on 20 and 24 May.
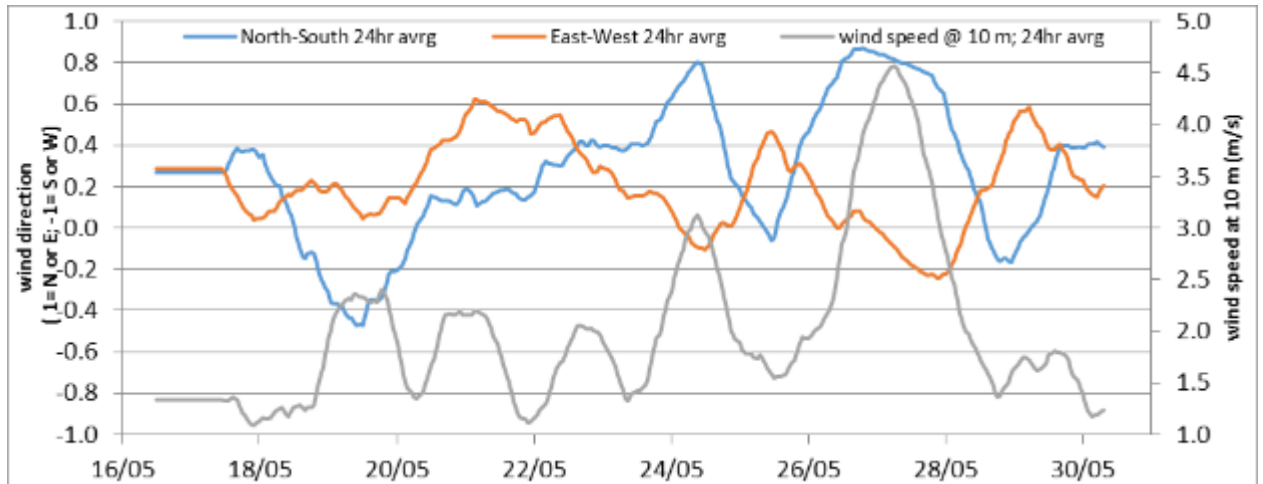
Figure 36. Moving average of wind speed and direction for the period where foil performance was monitored.

Figure 37 shows the accumulated R-values at the three positions. The accumulated R-values are similar to what was measured as part of SR202.
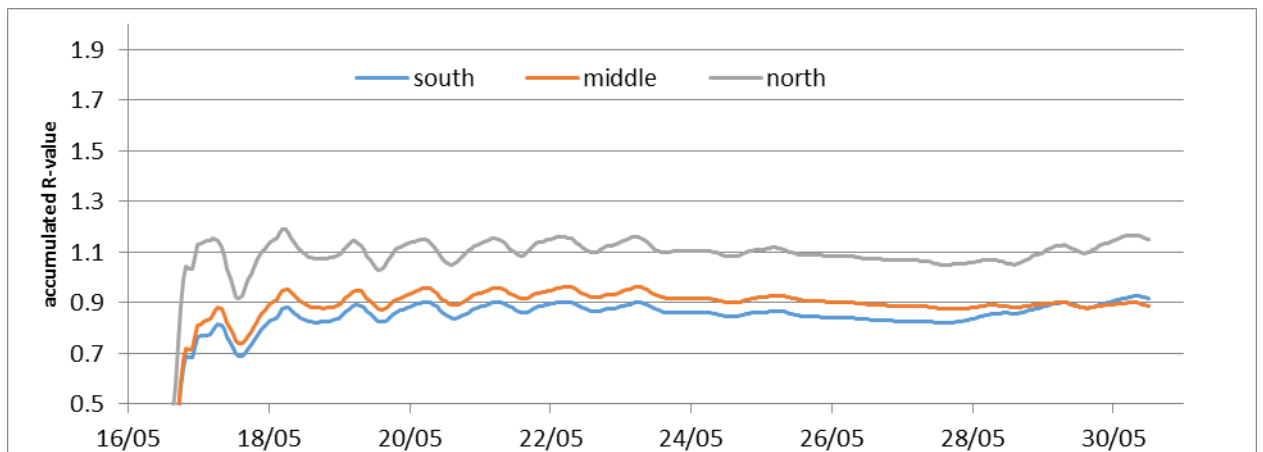
Figure 37. Accumulated R-value of foil insulation in three locations.

Comparing the two charts in Figure 36 and Figure 37 reveals that, although the R-values, when averaged over a period of a week or more, are consistent with the assumed performance of this type of floor system (under NZS 4214:2006 *Methods of determining the total thermal resistance of parts of buildings*), the performance over a period of 1 or 2 days can deviate significantly from those longer-term values.

The wind experienced over the second week of the monitoring period was much stronger and more sustained that what was experienced in the first week, but the accumulated R-value remains the same. Likewise, the day-to-day variation in R-value was much less during that first week.

These results also show that, apart from the sensors near the south and north walls on 29 and 30 May, the wind wash impact seems to be independent of location, and there does not seem to be a strong correlation with direction. This may simply be because of the small size (91 m²) of the floor.

Figure 38 and Figure 39 relate to the second week of data, with Figure 40–Figure 42 showing the data as a more detailed 1-hour moving average instead of the 1-day moving average in and for the wind data and R-value.
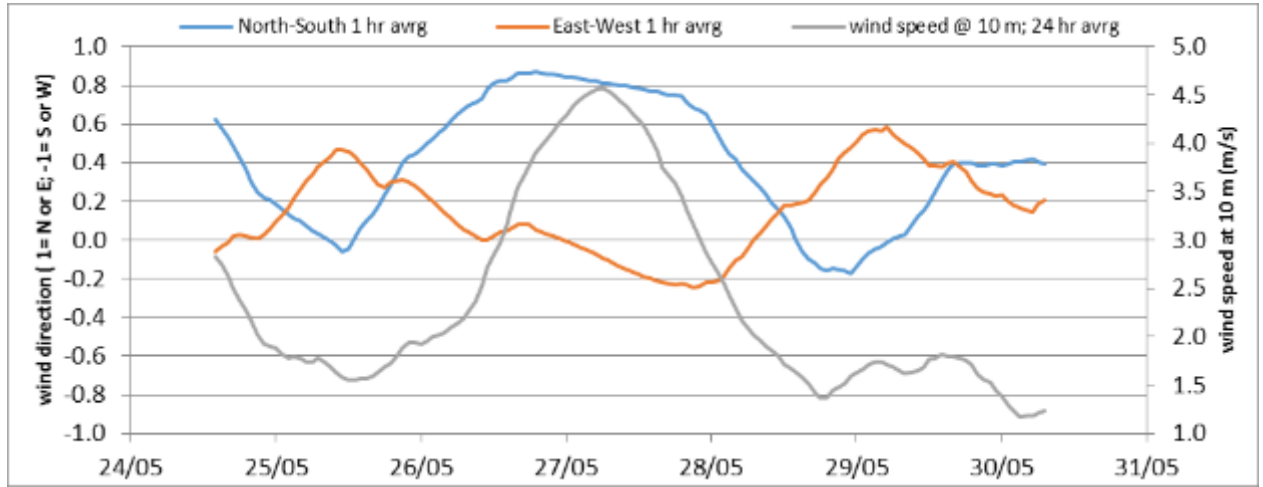
Figure 38. 24-hour average wind speed and direction for second week of monitoring foil insulation performance.
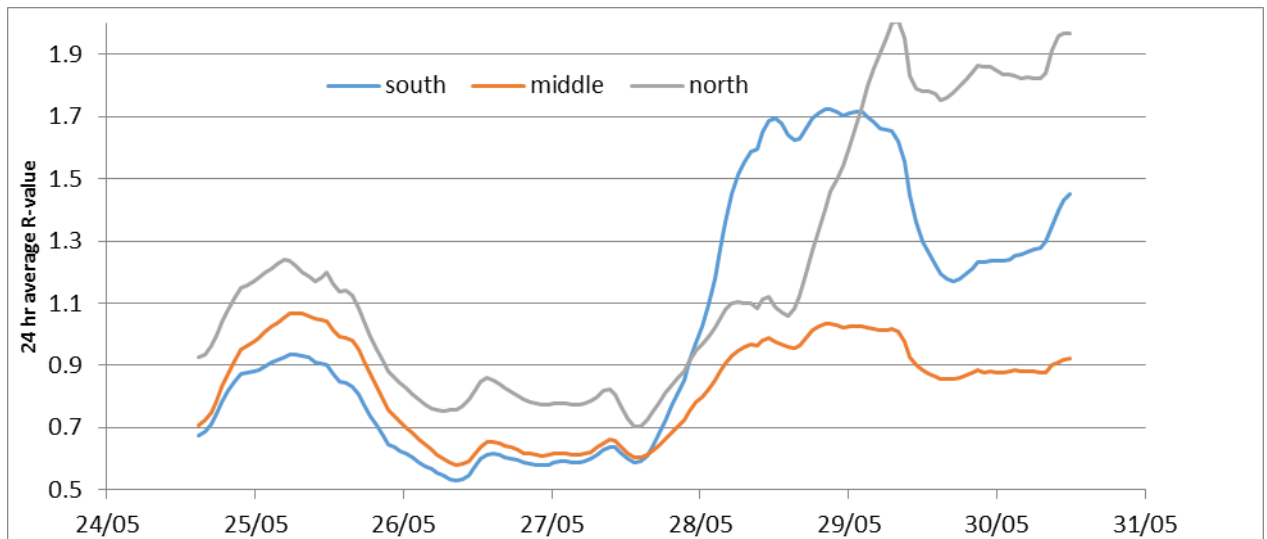
Figure 39. 24-hour average R-value of foil insulation in three locations – week 2.

Over the period 29–31 May, the wind velocity was only moderate, but there were significant changes in wind direction. The overall impact was that the R-value trend for the centre of the floor was a continuation of the data over the previous 2 weeks whereas there was an unusual increase in R-value at the two perimeter locations, first for the south and then for the north. The wind during that period swung around from north to the south then back again.

The big changes in R-value over that period highlight one of the limitations of foil insulation. During the hot afternoons, the performance of the foil was relatively good, but during the cold mornings when the insulation was needed most for foot comfort, the performance was relatively poor.
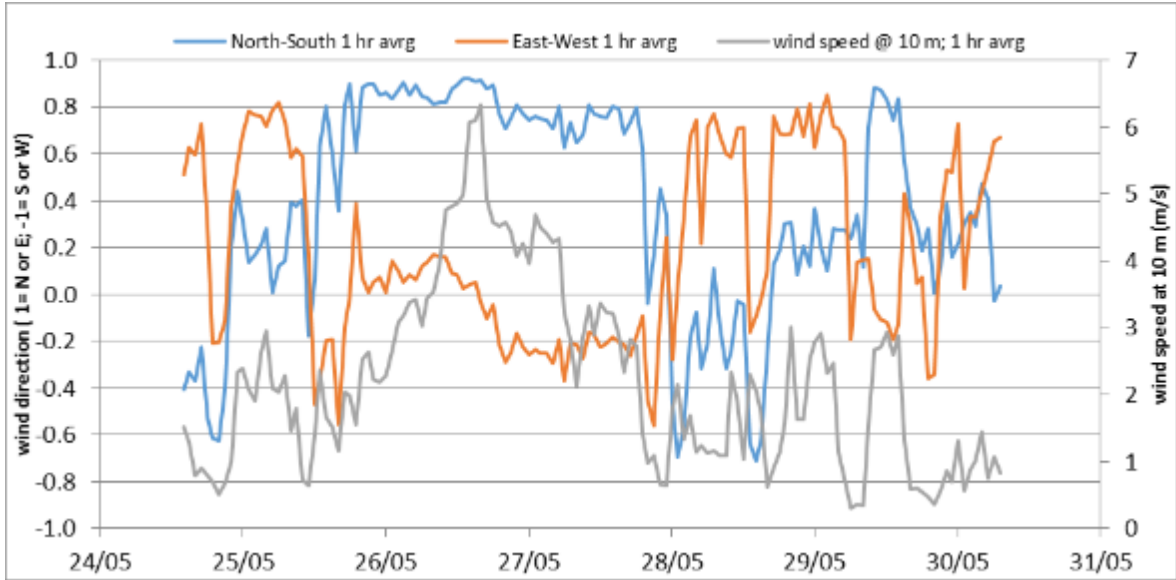
Figure 40. 1-hour average wind speed and direction for week 2 – foil insulation performance measurements.
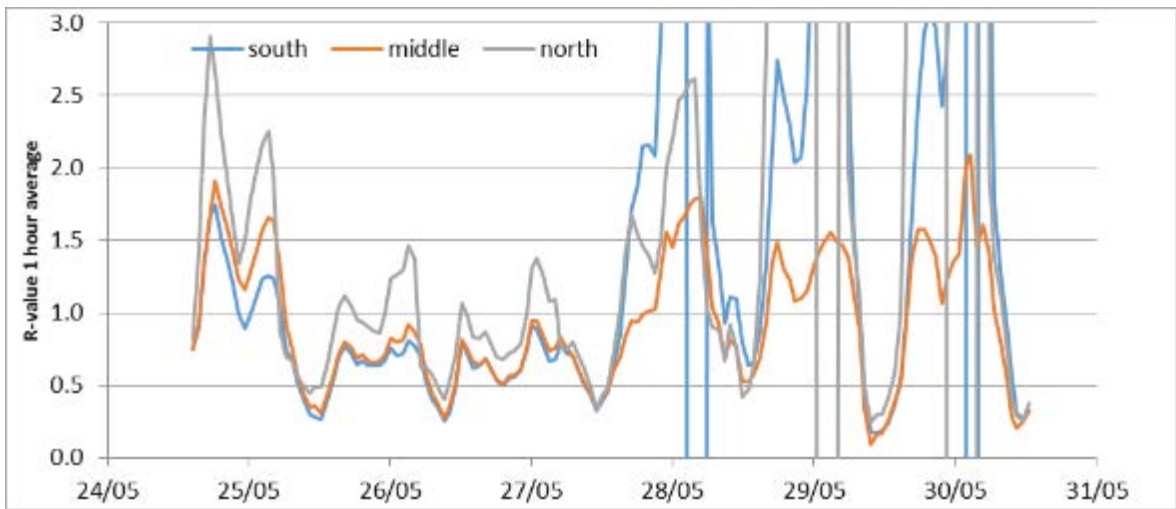
**Figure 41. 1-hour average R-Value for three locations – foil insulation.**
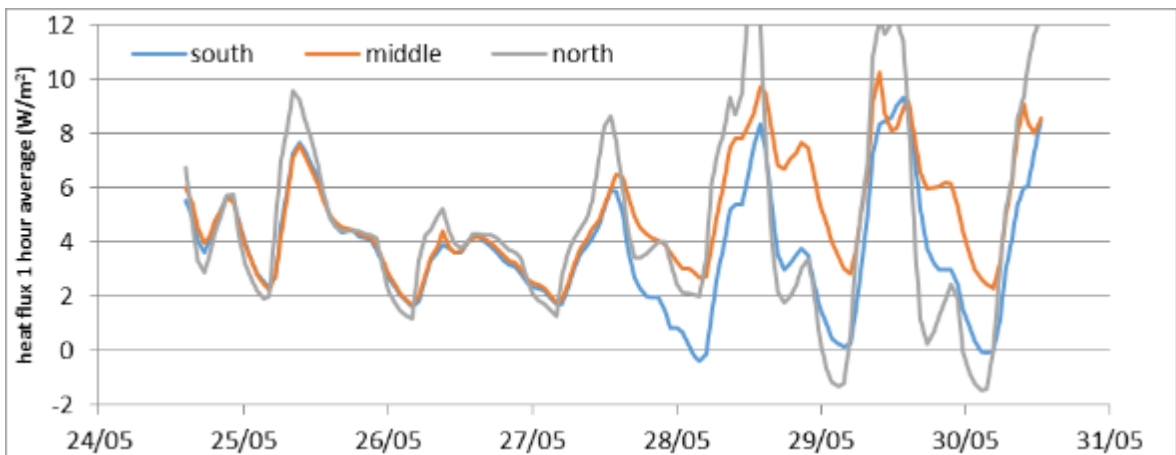

Figure 42. 1-hour average heat flux for three locations.

Figure 43 displays in detail the heat flow and temperature difference data for the sensor in the middle of the floor over the period 29–31 May. In the middle of the day on both 29 and 30 May, the heat flow gets out of sync with the temperature difference. After cold morning temperatures, the house begins to heat up. The heat flow responds almost immediately with the increase in temperature difference until midday when, for a few hours, the temperature difference beings to decrease without any change in the rate that the heat flow is increasing. After a couple of hours of decreasing temperature, the temperature difference starts increasing again.

At that point, the heat flow starts to decrease until around dusk when the trends reverse, temperature difference decreases and heat flow increases. At midnight, the heat flow starts to increase again and is in sync with temperature difference as external temperature drops until dawn and then increases again with the start of the next day.

A possible explanation for this behaviour is moisture condensing for a period on the surface of the foil then evaporating off again. It would also explain why the R-value increased more at the south and north locations than in the middle after the wind swung around from the north to the south and possibly cleared excess moisture from the airspace between the floor and the foil.
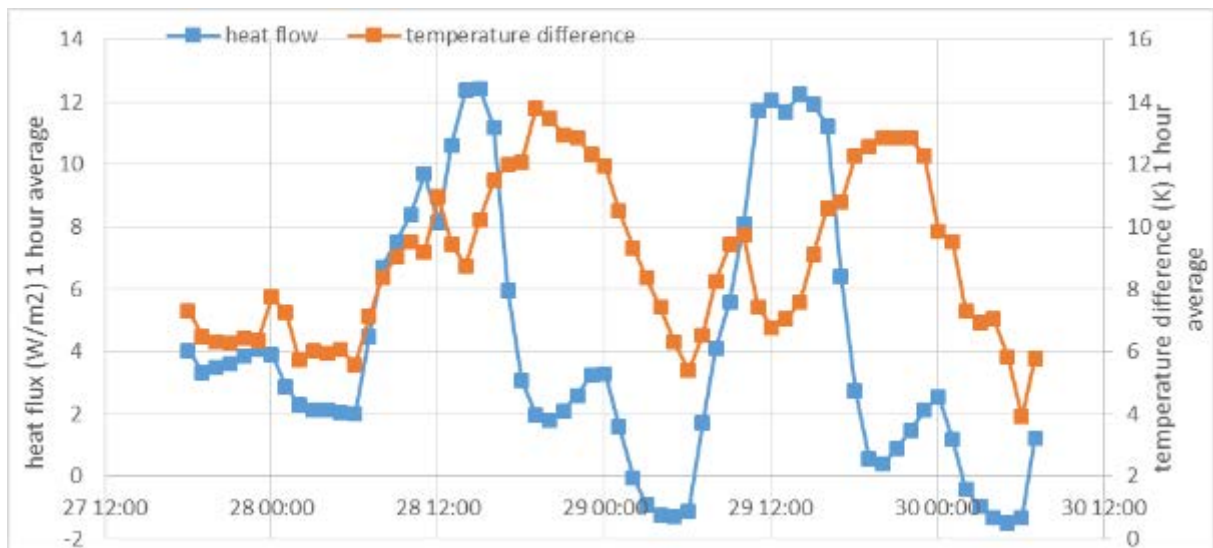
Figure 43. Heat flux and temperature difference in the middle of floor sensor location from 29–31 May.

Figure 44 shows the moving 24-hour average R-values at 1-hour intervals over the period 29–31 May. The R-value is plotted against air speed at 10 m. Air speed begins at 2.7 m/s with the R-values increasing as the air speed decreases to 1.5 m/s. The R-values then decrease as the air speed increases again to 2 m/s. The R-values do not decrease further as the air speed continues to increase to 4.5 m/s. The R-values start to increase again as the air speed drops below 3 m/s. Whilst the R-values at the north and middle locations return to the same values they were previously when the wind was at 1.5 m/s, the R-value for the south location is significantly higher.

Given that the air speed in the subfloor space is expected to be one-tenth of the value at 10 m, this result shows how sensitive the performance of draped foil is to wind speed.
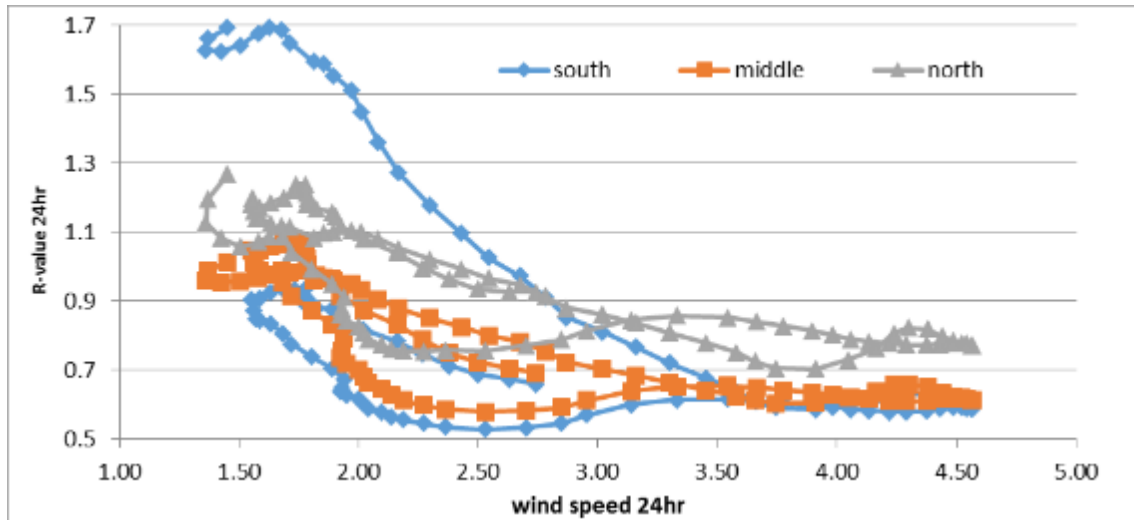
Figure 44. Progression of 24-hour moving average R-value of foil insulation from 29–31 May for three locations.

4.3.2 Determination of wind wash potential – bulk insulation

The thermal resistance of a representative selection of bulk underfloor insulation products was monitored for a 3-year period beginning in 2013. Wind velocity and direction were also measured, initially only at 10 m above ground, but in January 2015, a second sensor was added to measure wind speed and direction at ground level under the subfloor research building. Since in situ measurement of thermal resistance requires a sufficiently high temperature difference through the floor, the data analysis has been restricted to the calendar period of June through October.

Figure 45 to Figure 47 show a summary of the wind speed and direction data at ground level for June to October 2015. The prevailing wind direction is northerly, but there are also relatively frequent south-easterlies during the middle of winter. The strongest and most sustained winds with a daily average above 2.5 m/s are from the northerly direction, which is also the orientation of the floor joists.
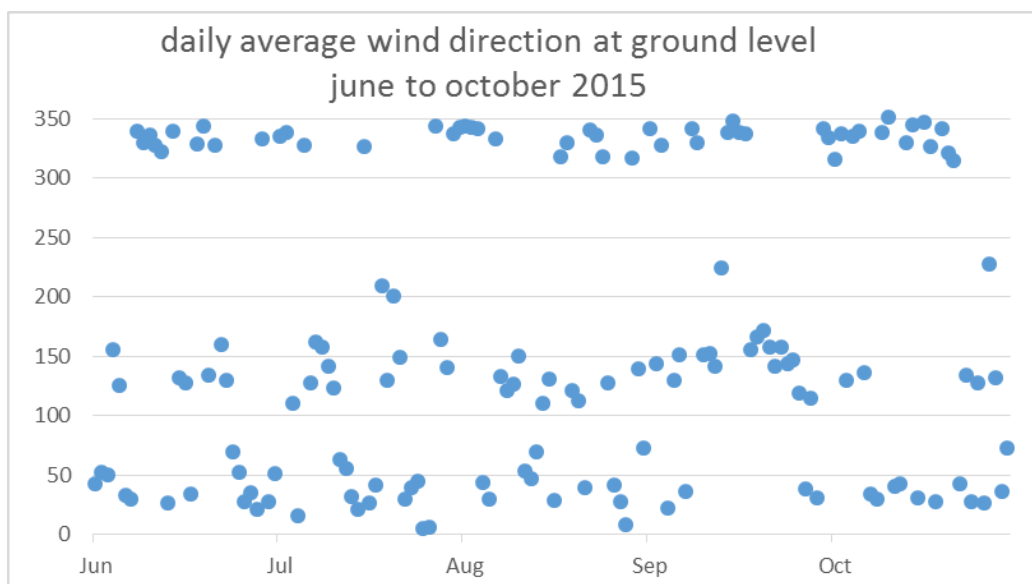
Figure 45. Daily average wind direction – winter 2015.
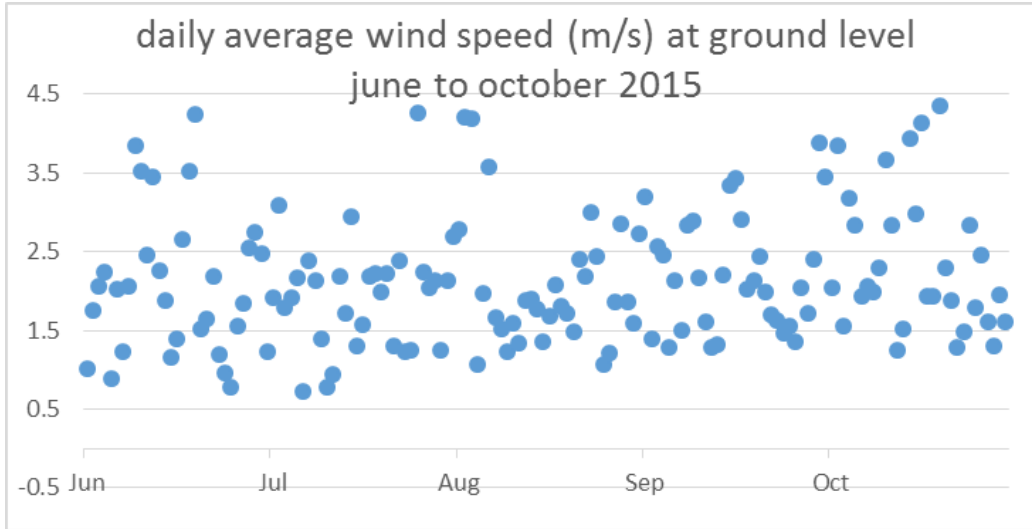
Figure 46. Daily average wind speed – winter 2015.
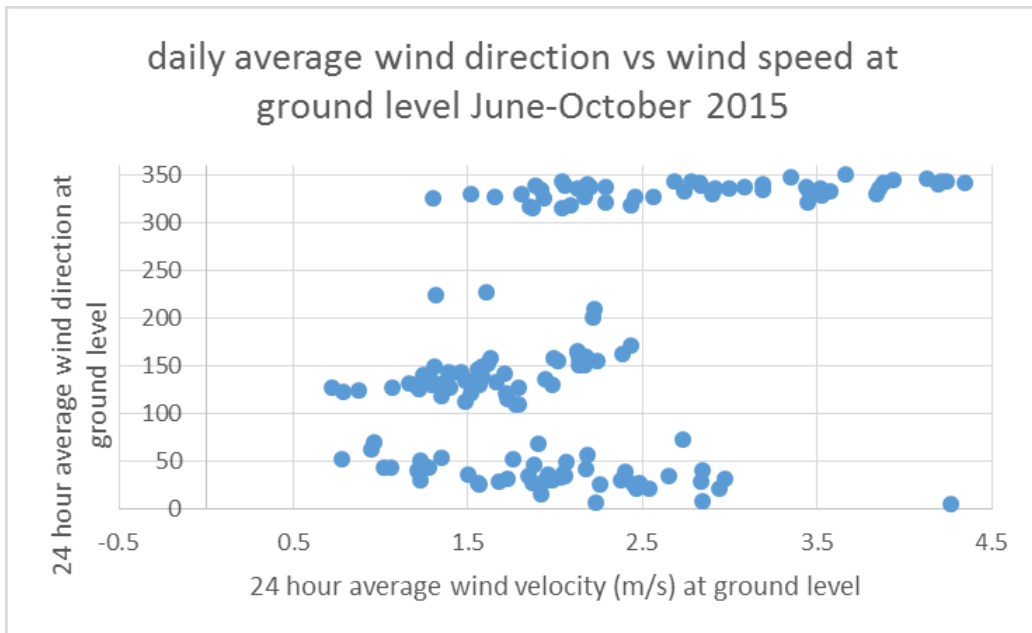
Figure 47. Daily average wind direction versus wind speed – winter 2015.

Figure 48 to Figure 51 show the frequency distribution of wind speed. The daily average is very rarely less than 1 m/s or more than 4 m/s and only occasionally above 3 m/s. Average daily wind speed for the 5 months from June to October is approximately 2 m/s. This also shows that the wind speed distribution for 2014 and 2015 were essentially the same.

Mostly, the daily average wind speed is in the range 1–3 m/s. When considering an hourly average, the maximum wind speed over the 5-month period was 7 m/s. From the raw data at 1-minute intervals, the maximum was 11.5 m/s in 2014 and 12.5 in 2015.
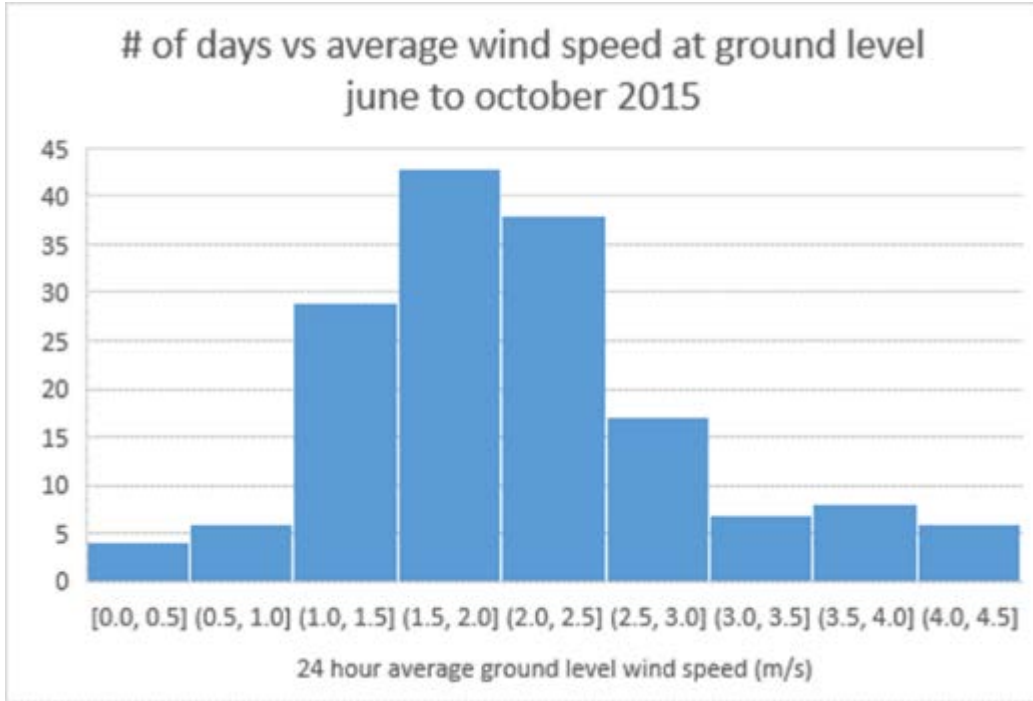
Figure 48. Daily average distribution of wind speed – winter 2015.

Figure 49. Percentage of time above a given ground level wind speed – winter 2015.
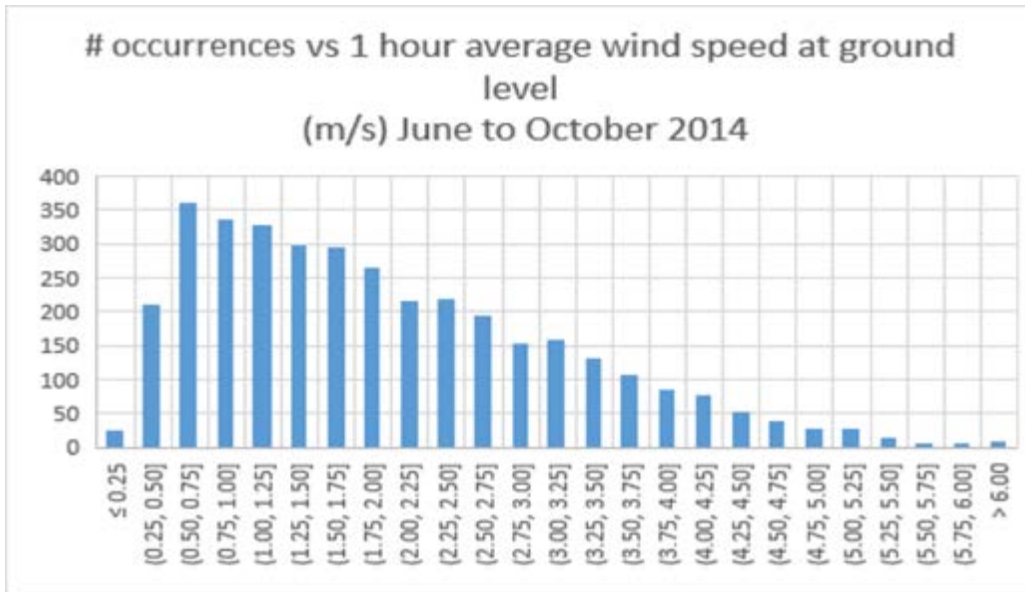
Figure 50. Distribution of 1-hour average ground level wind speed – winter 2014.
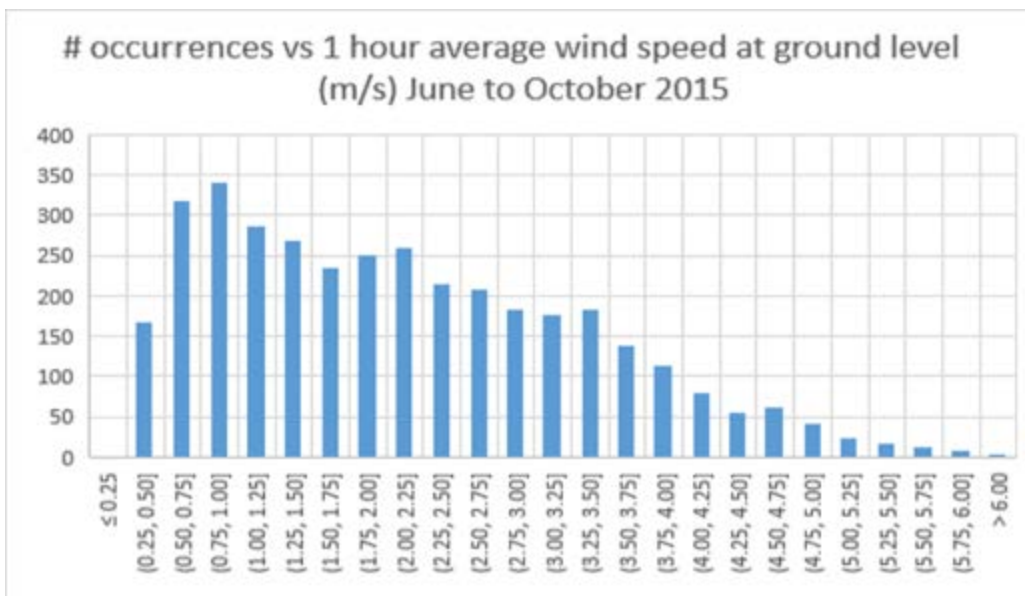
Figure 51. Distribution of 1-hour average ground level wind speed – winter 2015.

Whilst the exposure to wind of the subfloor area of the subfloor research building is not necessarily a worst case, the subfloor orientation and geographic location (greater Wellington region), along with the rural setting, is assumed to subject the insulation products to significantly more wind wash than occurs for most suspended timber floors in New Zealand.

Figure 52 to Figure 57 present a selection of the results for thermal resistance plotted against wind speed for the 5 winter months of either 2014 or 2015. The R-values are system values and so are typically higher than the actual R-value of the insulation material alone. Comparing the average R-value of the various products or comparing measurements against the theoretical system value is not necessarily meaningful. The purpose of the measurements was to assess the impact of wind wash on representative material types ranging from air impermeable (rigid foams) to highly air permeable (low-density fibrous).
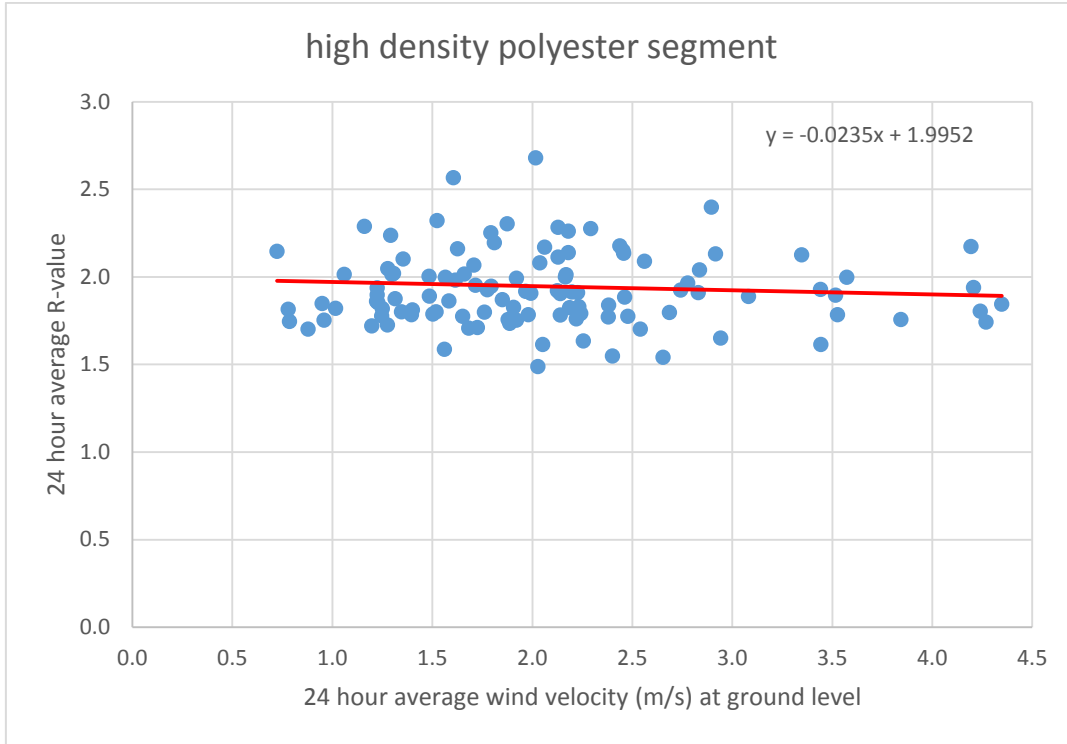
Figure 52. 24-hour average R-value versus wind speed – high-density polyester segment (2014 data).
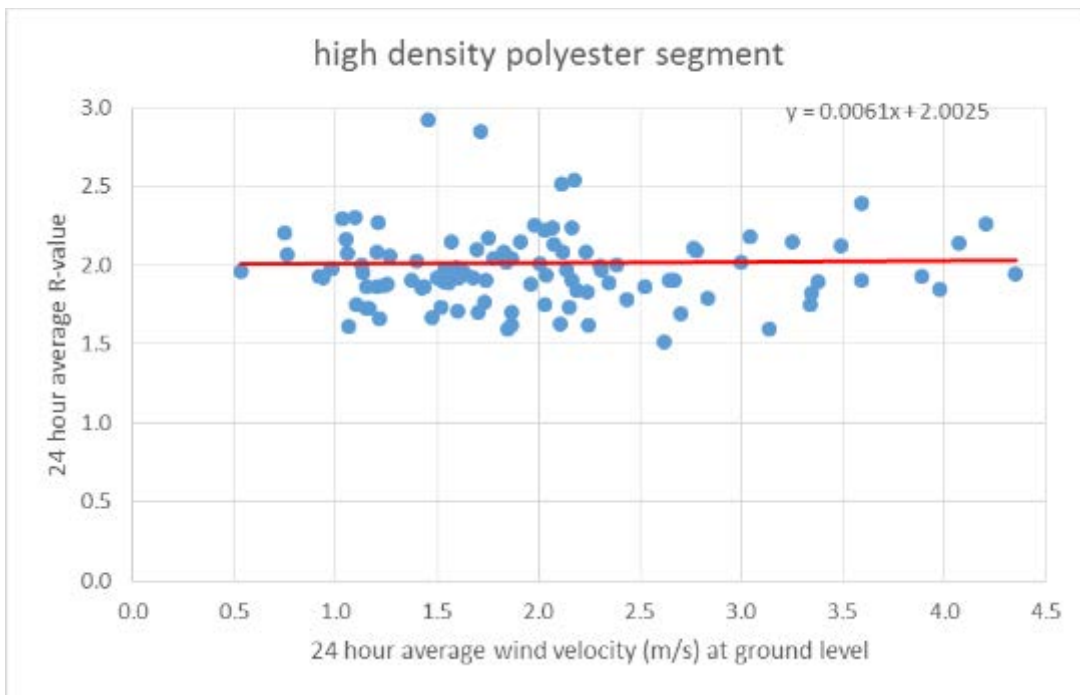
Figure 53. 24-hour average R-value versus wind speed – high-density polyester segment (2015 data).
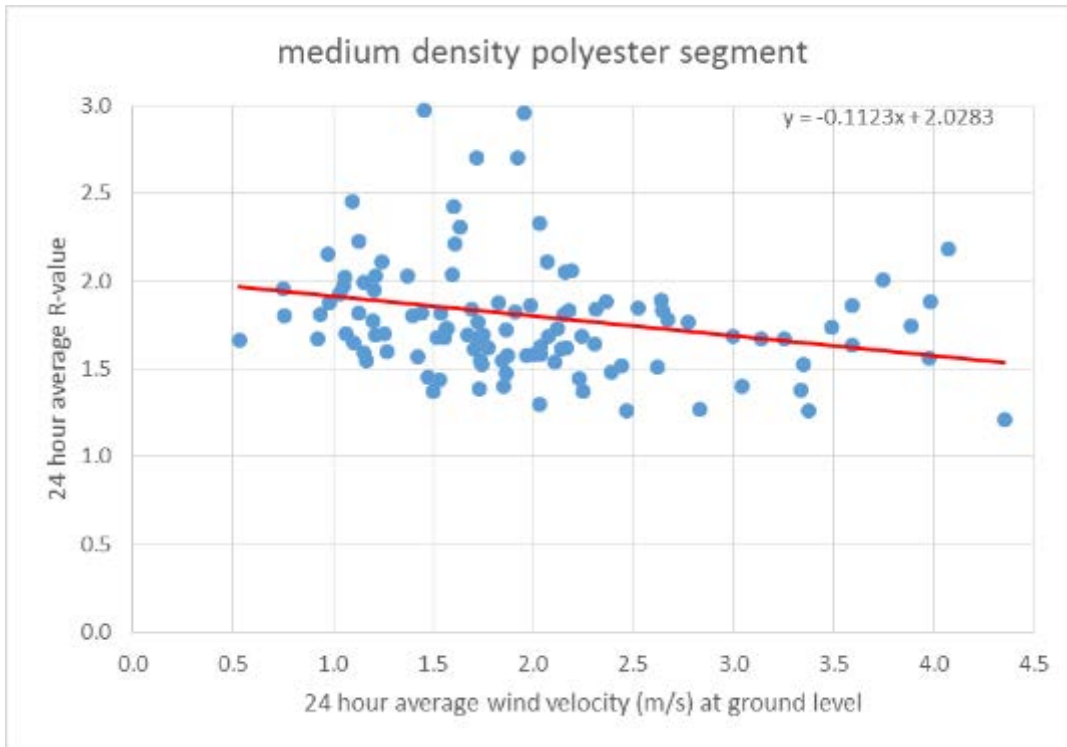
Figure 54. 24-hour average R-value versus wind speed – medium-density polyester segment.
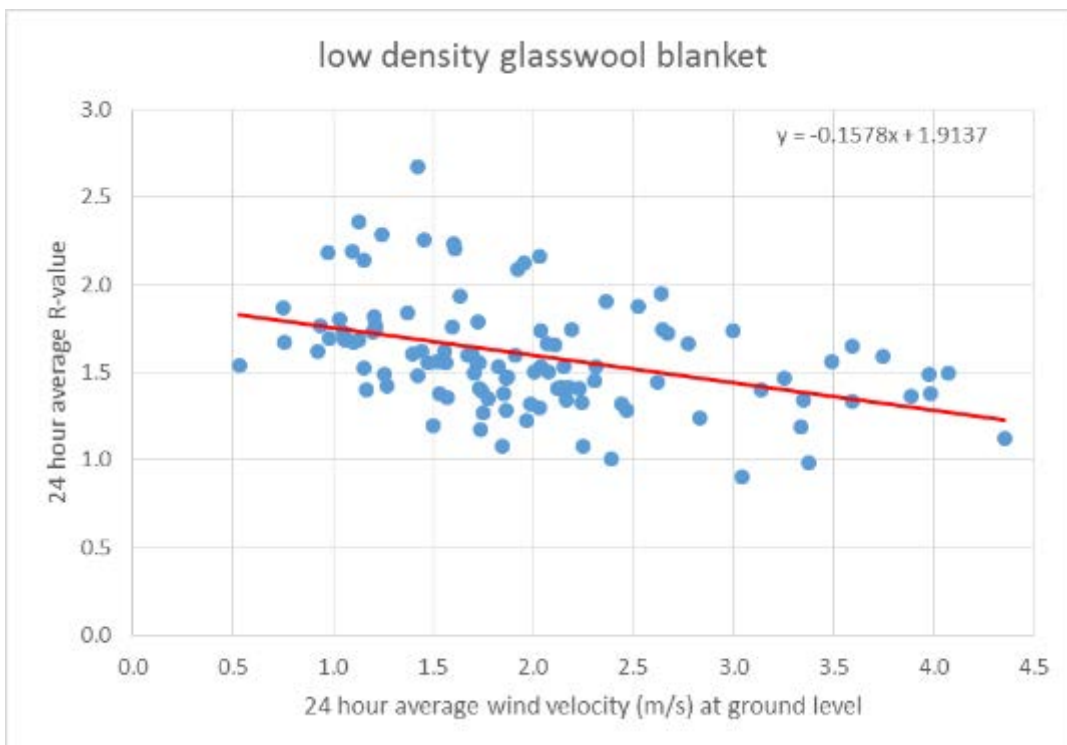
Figure 55. 24-hour average R-value versus wind speed – low-density glasswool blanket.
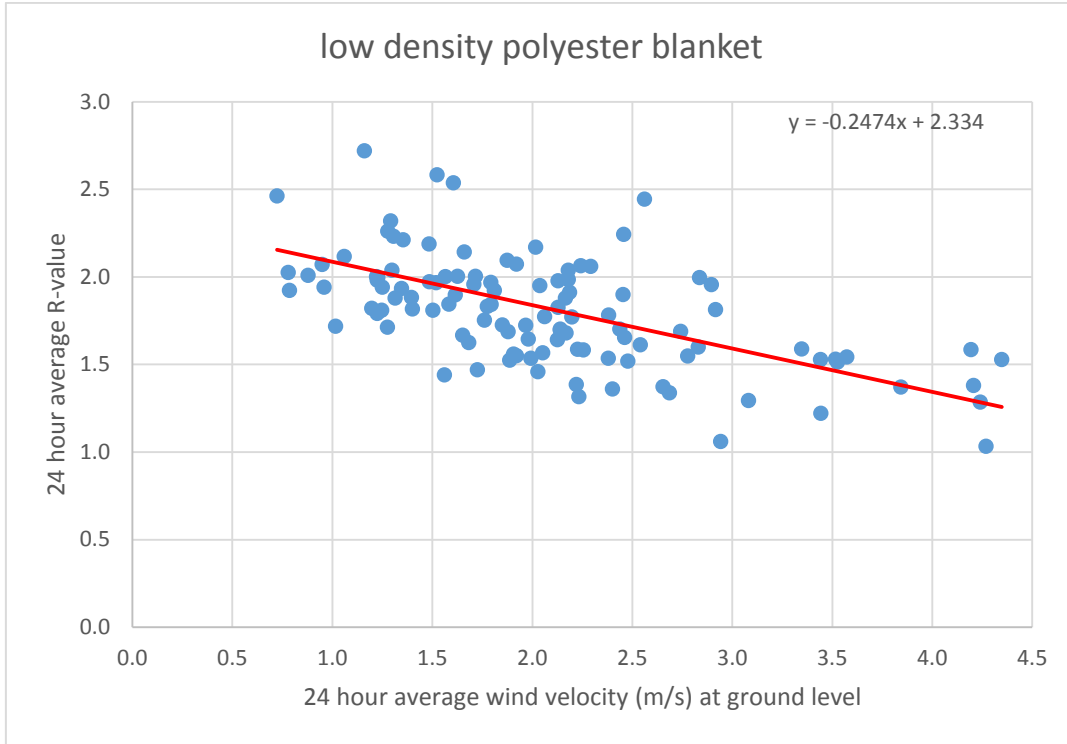
Figure 56. 24-hour average R-value versus wind speed – low-density polyester blanket (2014 data).
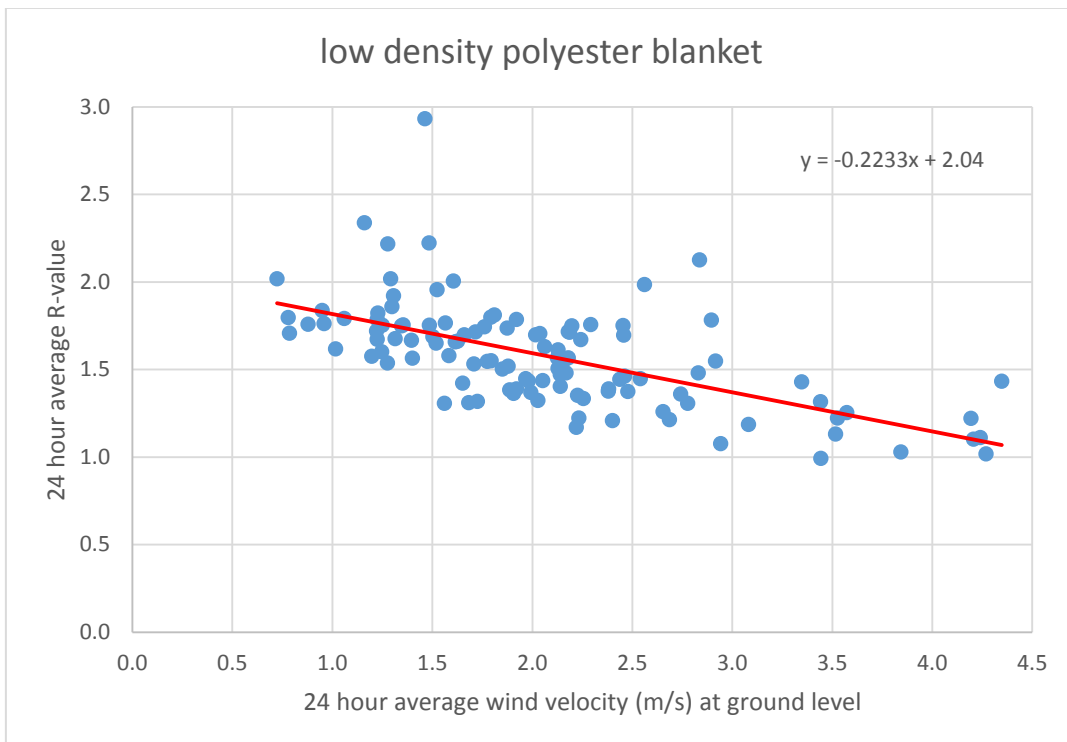
Figure 57. 24-hour average R-value versus wind speed – low-density polyester blanket (2015 data).

A detailed analysis of the data could not detect a significant impact on thermal resistance of average daily wind velocity up to 1 m/s, even for the low-density fibrous materials. Above that wind speed, the impact on a percentage of the still air R-value was roughly linear for the medium and low-density fibrous products.

Whilst a short-term burst of very strong wind can have a temporary impact on the heat flow through or around the medium and high-density fibrous products and the rigid foam (EPS), the impact on the longer-term average R-value was negligible and below the resolution of the measurements.

Only the medium and low-density fibrous materials were significantly affected by wind wash. The linear best fit for the low-density glasswool data reveals a 9% decrease in R-value for a 1 m/s increase in average wind speed. The value for the two low-density polyester products is similarly 12% for every 1 m/s increase. A conservative approach to the thermal rating of the low-density fibrous products would be to assume that the average wind velocity in the subfloor space is a high exposure value of 2 m/s and the system R-value is correspondingly 12% less than what it would be without the wind wash. Good thermal design would be to increase the R-value of the insulation material by 12% and to add on a further 12% (24% total increase) to account for the 15% of time when the average wind velocity may go above 3 m/s. Under that regime, an R1.9 low-density fibrous insulant could be assumed to perform as effectively as an R1.5 medium or high-density insulant.

4.3.3   In-service observation of durability

After completion of the thermal resistance measurements of the draped foil in the ventilation research building in May 2012, bulk insulation material was installed by leaving the foil in place and pushing it up and holding it against the underside of floor with the bulk insulation. The bulk insulation was a mixture of both medium and high-density polyester underfloor insulation products with thicknesses of approximately 90 mm. The insulation was held in place by friction fit with some cut to size to exactly fit the joist spacing and some wider than the joist spacing and folded down along one edge. The subfloor space was left open for the following 12 months without any of the insulation becoming dislodged.

Over the same period, the subfloor space of the subfloor research building was also left fully exposed. The insulation materials under the subfloor research building included the medium and high-density 90 mm products as well as thicker high-density polyester material and low-density polyester blanket. Friction fitting followed the same regime as for the ventilation research building except the existing draped foil insulation was removed before installing the bulk insulation. The thick polyester products were cut to the joist width and friction fitted, and the low-density blanket was stapled in place as per normal installation practice. All of the insulation material installed under the floor remained in place over the 12 months of wind exposure.

4.3.4   Moisture

In June 2013, the subfloor space of the ventilation research building was enclosed without polythene ground cover, but the access door was left open until December 2013. Once the access door was closed, the air became saturated and moisture droplets formed on the bottom face of the insulation. The moisture droplets were present all through the remaining months of summer and autumn until vents were added to the floor in May 2014.

It was not practical to conduct in situ thermal resistance measurements over those 5 months, but samples of both the low and high-density insulation materials were removed and tested for moisture content and thermal conductivity.

The samples were immediately weighed and thermal resistances measured before drying and remeasuring. There was no change in weight of the two samples after drying, so it was assumed that the act of removing the samples from the floor must have been sufficient to knock the moisture droplets off the surface of the insulation and that the moisture had not accumulated within the body of the insulation. Likewise, there was no change in thermal resistance after drying the two samples.

At the start of summer 2013, half of the subfloor research building floor was enclosed but without adding polythene ground cover. The enclosed part of the floor included samples of medium and high-density polyester, low-density polyester blanket and low-density glasswool blanket. Because the flooring of the subfloor research building was less airtight than the floor of the ventilation research building, the air in the subfloor space did not reach saturation until the indoor air temperature was lowered from 20°C to 18°C at the start of winter 2014. At that point, a thin layer of moisture could be felt, but not seen with the naked eye, on the underside of all of the insulation in the enclosed floor area. After almost 2 years of exposure to subfloor air above 95% relative humidity, there has been no detectable increase in weight or moisture content of any of the insulation samples, although the underside of the insulation has remained slightly damp.

In situ measurements of thermal conductivity over the 2 years showed that the thermal resistance of the test samples did not significantly change. Concurrent measurements of thermal resistance of identical samples in the non-enclosed area of the floor that was exposed directly to wind showed that wind wash was more of an issue than elevated subfloor relative humidity.

5. Summary

5.1 Corrosion

Based on observations and measurements obtained within the corrosion part of this research, the following could be derived:

- The environment of subfloors with typical construction is more benign than the atmosphere surrounding the house. The corrosion rate of mild steel when exposed to the subfloor could be at least seven times lower. This is partly because the subfloor is not directly subjected to weather conditions, such as rain, and is sheltered to a certain extent from aggressive media such as sea salt and dirt.
- The samples close to vents generally corroded faster than those installed in corner and centre locations of the same subfloor. The difference could be significantly increased when natural ventilation provided to the subfloor is increased, for example, by using timber planks rather than concrete perimeter foundation walls as subfloor enclosures. The local environment close to a vent normally has a larger variation of temperature and humidity, which could increase condensation on metal surfaces. Further, metal surfaces could be wet by rainwater splash when timber planks with wide gaps are used for subfloor enclosure construction. Occupier actions can also have a significant effect here, for example, landscaping works can lead to additional liquid water entering through vents.
- Ground soil condition has influences on deterioration of metallic components used for subfloor construction. Wet soil could produce moisture that is detrimental to metal durability. Ground coverage could, to a certain extent, prevent transfer of moisture from wet soil to the subfloor space. An increase of air exchange by increasing vent dimension could decrease the chance of humid air staying in the subfloor space for longer periods. These two aspects could then benefit material performance.
- Metals sandwiched into timber blocks showed very low mass losses due to corrosion in this study. This is indicating that the timber blocks exposed to these subfloors did not hold moisture higher than the threshold (>20%) for longer periods to trigger fast corrosion.

5.2 Moisture and ventilation

Given the results presented here, the following can summarise the moisture side of the project:

- An airtight subfloor (or with a low ventilation area) is detrimental to the building and occupants as significant accumulation of moisture can occur in a relatively short period of time.
- Adding ventilation openings is relatively easy to accomplish, and openings equivalent to the Acceptable Solution E2/AS1 of 3,500 mm^2/m^2 are sufficient to remove the potential moisture evaporating from the soil. The Acceptable Solution does given some additional drying capacity, which provides a reasonable safety margin. It must be stressed that the research buildings under investigation here were very well exposed and consequently had a higher achieved ventilation rate than what is likely in a suburban environment.
- Polythene ground covers are an effective means of source control and are a useful addition to available ventilations options for dealing with subfloor moisture.

However, access can be an issue when applying a ground cover, particularly with older buildings built close to the soil. In addition, polythene ground covers should be detailed such that they do not provide a space for rainwater to accumulate.

- The observed patterns of moisture accumulation indicate that the southern side of a building is more likely to suffer moisture issues and that any inspection or judgement made on the subfloor of a building should be sure to consider the entire space and not just the area in the vicinity of the subfloor access.

5.3   Insulation performance

The two main questions at the start of this project regarding insulation performance in the subfloor space were how much impact does subfloor moisture have on insulation performance, and what effect does wind wash have on the installed R-value of subfloor insulation?

- The measurements of the impact of moisture accumulation in the insulation on insulation R-value demonstrated that the effect is negligible. By the time specimens that had accumulated moisture were measured in the BRANZ heat flow meter, the moisture had disappeared, and no difference was measureable between a wet or dry specimen. In the case of accumulation due to water vapour in the subfloor, this tended to be on the lower surface of the insulation and would form droplets and fall off before a significant accumulation could occur.
- The work verified the performance (or lack thereof) of draped foil insulation, particularly when it was windy or relatively cold, demonstrating that bulk insulation products are superior.
- The wind wash effect on a variety of insulation products was measured with respect to wind speed, and the following points can be made:
    o In an exposed subfloor with a low-density bulk insulation product, there is an effect that can be correlated to wind speed. However, this can be counteracted with a 25% increase in installed R-value.
    o In an exposed subfloor with a medium (or greater) density bulk insulation product, there is minimal effect on the average system R-value.
    o In general, enclosing the subfloor and using ventilation provisions conforming to Acceptable Solution E2/AS1 will mean that even lower-density products will retain their performance.

References

Buckett, N., Marston, N., Saville-Smith, K., Jowett, J. and Jones, M. (2011). *Preliminary BRANZ 2010 House Condition Survey Report*. Study Report SR240, BRANZ Ltd, Judgeford, New Zealand.

Clark, S., Cox-Smith, I. (2008). In-situ measurement of thermal resistance for suspended timber floors. Study Report SR202, BRANZ Ltd, Judgeford, New Zealand.

Ficco, G., Iannetta, F., Ianniello, E., d'Ambrosio Alfano, F. and Dell'Isola, M. (2015). U-value in situ measurement for energy diagnosis of existing buildings. *Energy and Buildings*, 104, 108–121.

Jensen, L. (1986). Determination of leakages in the building envelope using pressurization test measurements. *Air Infiltration Review*, 7 (4), 6–8.

Jones, M. and Page, I. (2005). New Zealand 2005 House Condition Survey. Study Report SR142, BRANZ Ltd, Judgeford, New Zealand.

Marston, N., Jones, M. (2014). *BRANZ House Condition Survey*. Building a Better New Zealand, 3-9 September 2014, Auckland.

Page, I., Sharman, W. and Bennett, A. (1995). New Zealand House Condition Survey 1994. Study Report SR62, BRANZ Ltd, Judgeford, New Zealand.

Straube, J., Onysko, D. and Shumacher, C. (2002). Methodology and design of field experiments for monitoring the hygrothermal performance of wood frame enclosures. *J Thermal Env & Bldg Sci,* 26 (2), 123–151.

Appendix A: House details – field survey

A.1 House 1 – Auckland

Construction	Concrete perimeter foundation wall and brick veneer wall cladding – see Figure 58 and Figure 59
Underfloor insulation	R1.5 polyester
Subfloor ground	Covered with black polyethylene sheet
Configuration/dimensions	See Figure 60
Ventilation	22 in total vents with a dimension of 200 × 130 mm – each has 20 holes of 20 × 30 mm
Testing arrangement	Steel samples and sensors were installed at seven locations as shown in Figure 60
Monitoring period	4 June 2013 to 4 June 2014

Figure 58. House 1 exterior.


Figure 59. House 1 subfloor space.
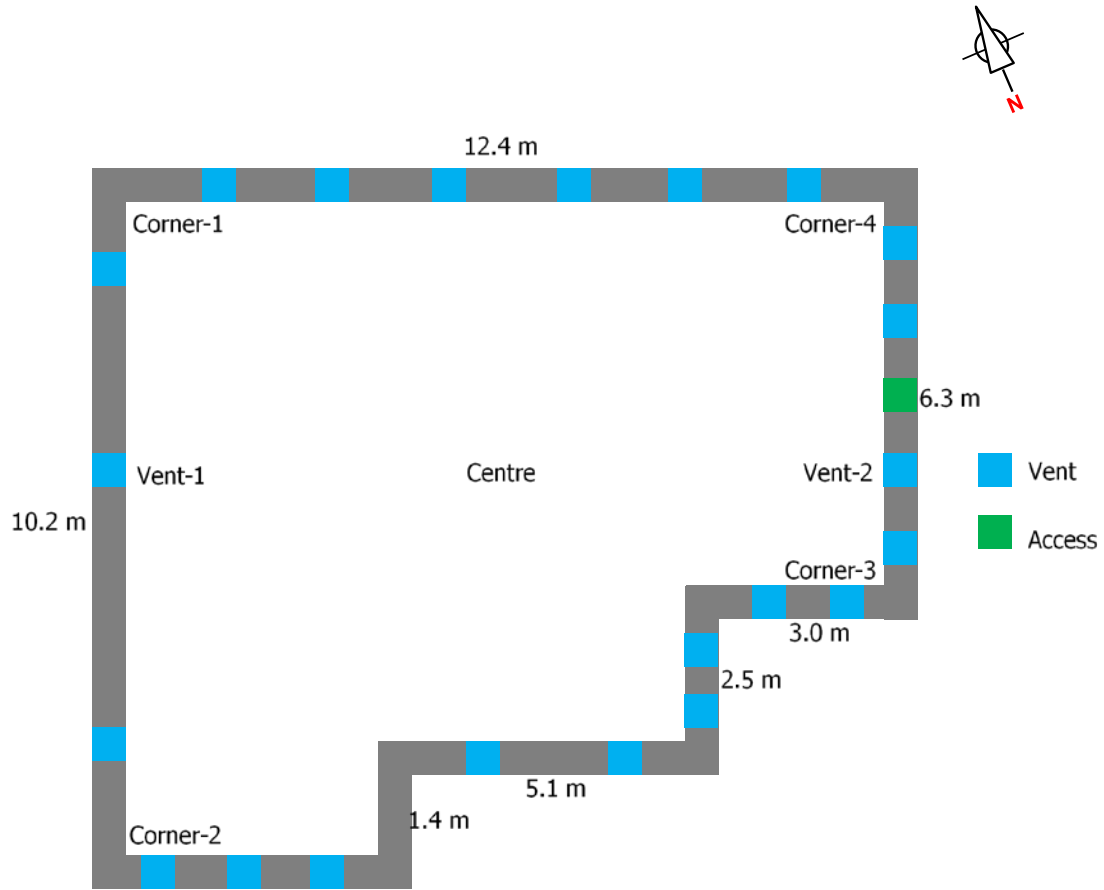
Figure 60. Dimensions of subfloor and sample arrangement of house 1.

A.2 House 2 – Auckland

Construction	Brick/concrete foundation wall, fibre-cement weatherboard – see Figure 61 and Figure 62
Underfloor insulation	R1.6 glass fibre
Subfloor ground	Not covered, appeared dry in most areas with some parts with relatively soft and wet soil
Configuration/dimensions	See Figure 63
Ventilation	16 in total vents with a dimension of 380 × 160 mm – each has 55 holes of 22 × 22 mm
Testing arrangement	Steel samples and sensors were installed at seven locations as shown in Figure 63
Monitoring period	4 June 2013 to 4 June 2014

Figure 61. House 2 exterior.
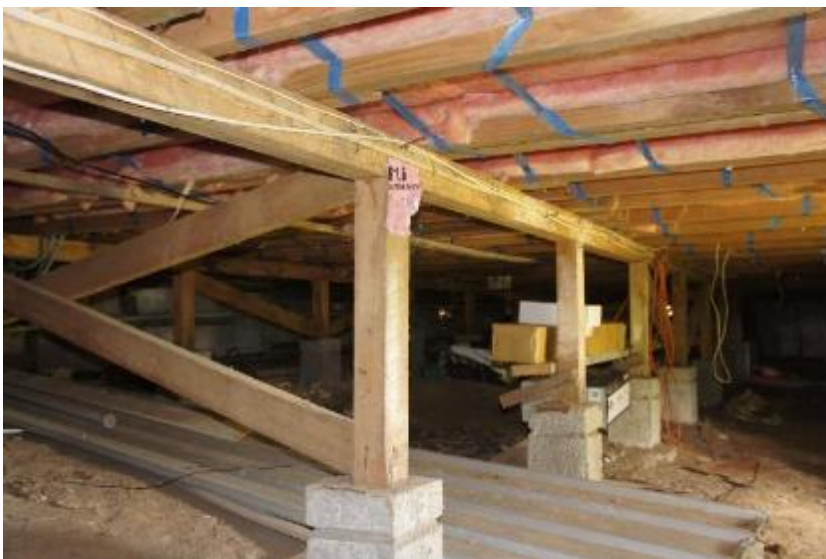
**Figure 62. House 2 subfloor.**
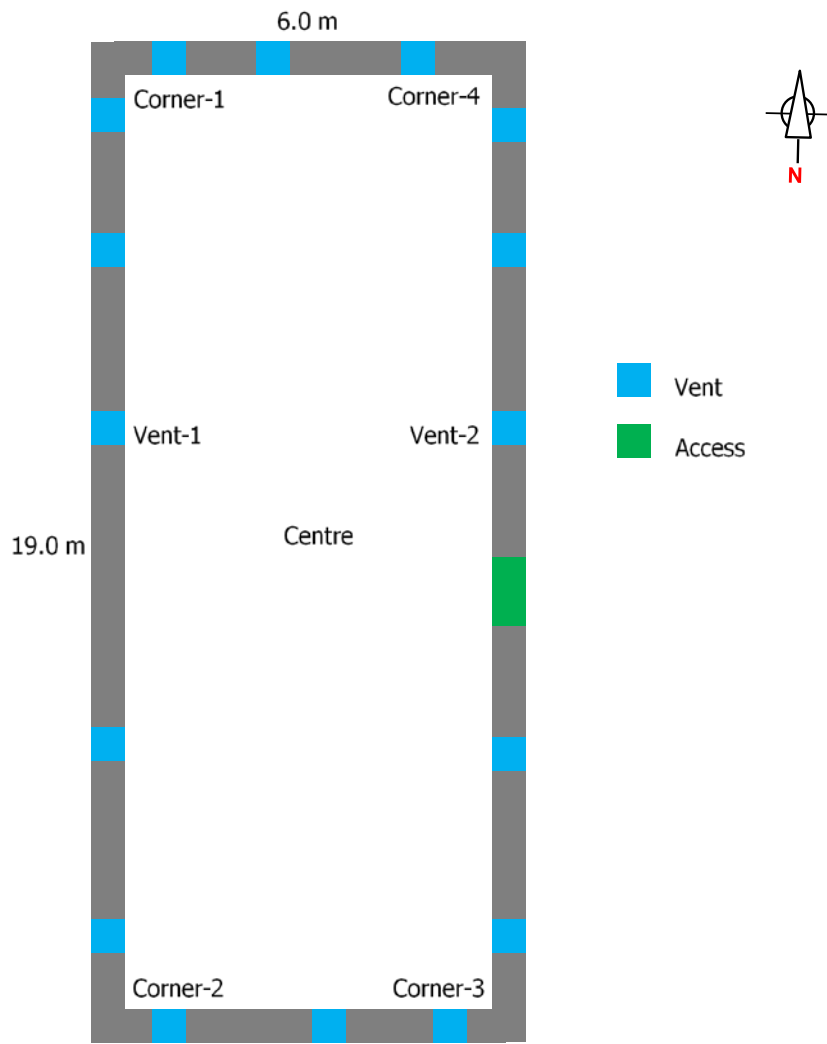
Figure 63. Dimensions of subfloor and sample arrangement of house 2.

A.3 House 3 – Auckland

Construction	Perimeter concrete foundation wall, weatherboard – see Figure 64 and Figure 65
Underfloor insulation	R1.5 polyester
Subfloor ground	Covered with black polyethylene sheet, soil was wet, underground water visible in trench along foundation wall in winter season
Configuration/dimensions	See Figure 66
Ventilation	13 vents (only for tested subfloor section) with a dimension of 160 × 100 mm – each has 20 holes of 25 × 15 mm
Testing arrangement	Steel samples and sensors were installed at seven locations as shown in Figure 66
Monitoring period	5 June 2013 to 5 June 2014

**Figure 64. House 3 exterior.**

Figure 65. House 3 subfloor.
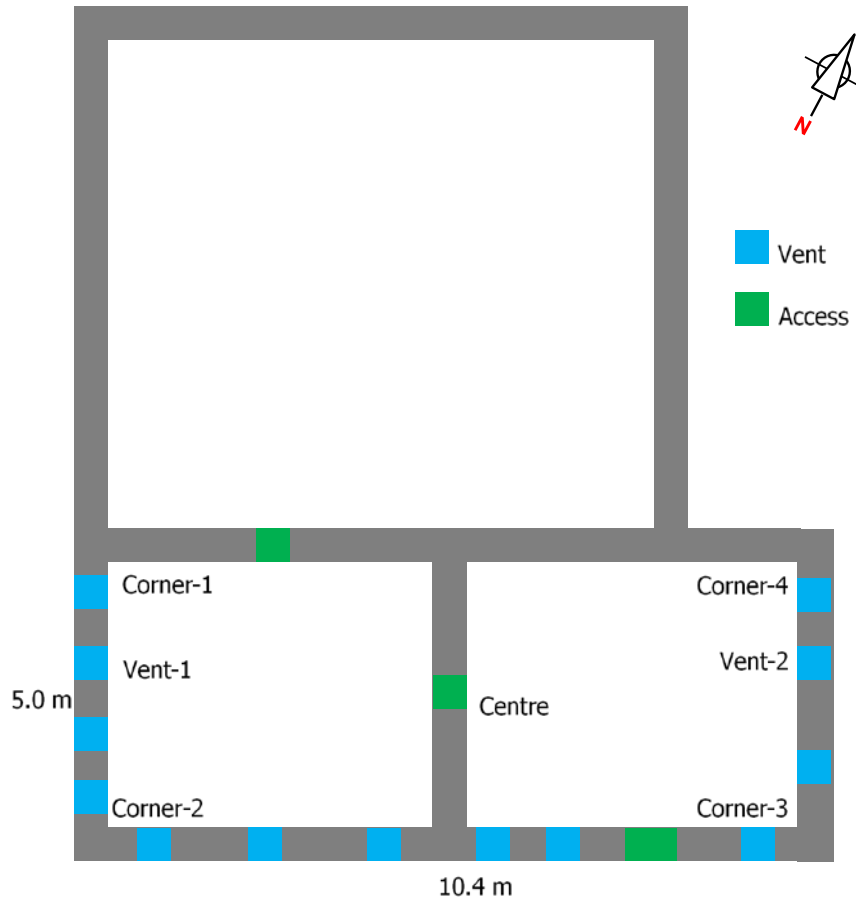
Figure 66. Dimensions of subfloor and sample arrangement of house 3.

A.4 House 4 – Wellington

Construction	Perimeter concrete foundation wall, brick veneer wall cladding – see Figure 67 and Figure 68
Underfloor insulation	R1.5 polyester
Subfloor ground	Covered with black polyethylene sheet
Configuration/dimensions	See Figure 69
Ventilation	19 vents in total with a dimension of 180 × 120 mm – each has 15 holes of 20 × 20 mm
Testing arrangement	Steel samples and sensors were installed at seven locations as shown in Figure 69
Monitoring period	20 May 2013 to 20 May 2014

Figure 67. House 4 exterior.

Figure 68. House 4 subfloor.
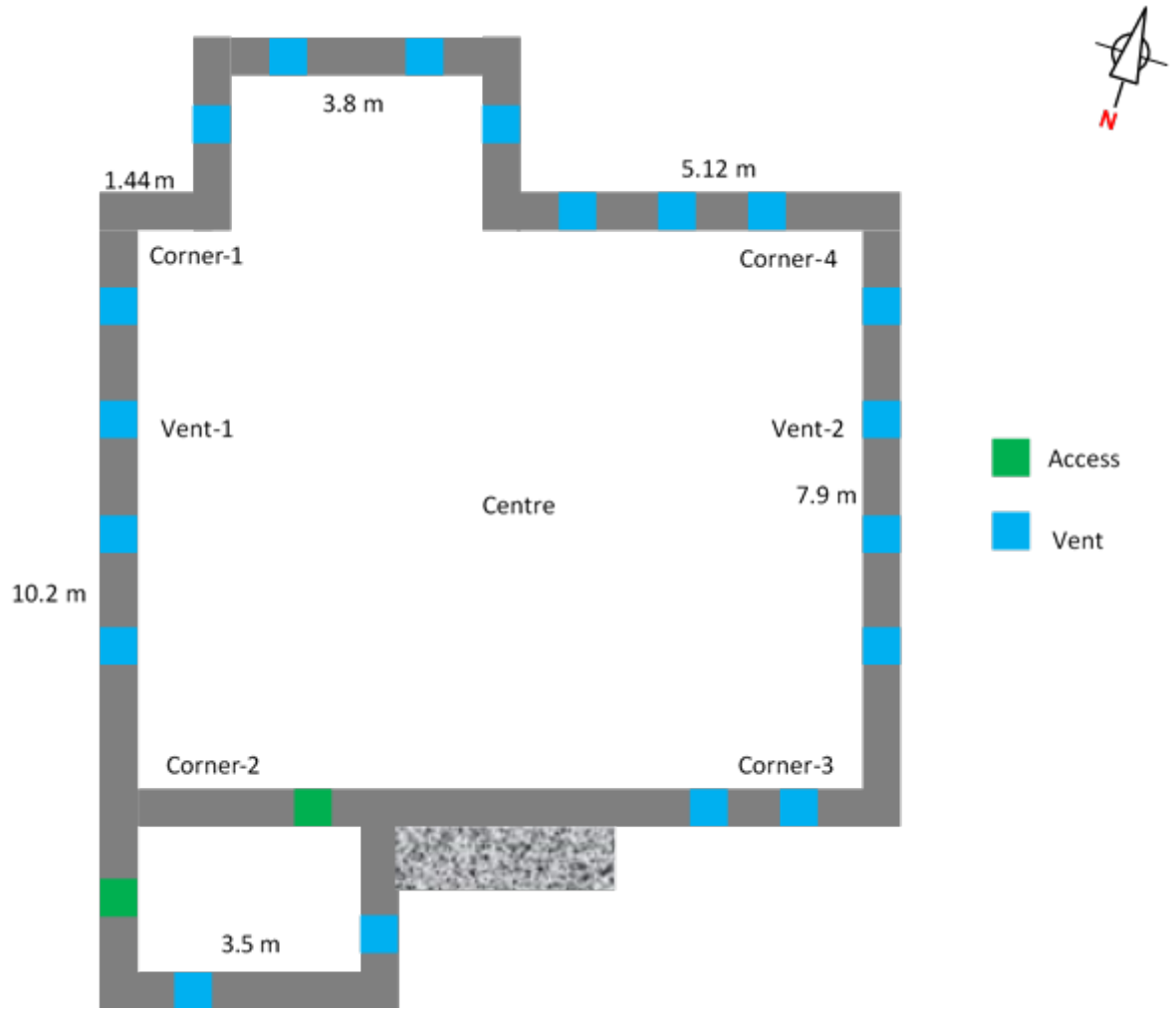
Figure 69. Dimensions of subfloor and sample arrangement of house 4.

A.5 House 5 – Wellington

Construction	Concrete corner with timber planks, weatherboards – see Figure 70 and Figure 71
Underfloor insulation	Polystyrene
Subfloor ground	Very wet (with water ponding in rainy season) and not covered
Configuration/dimensions	See Figure 72
Ventilation	10–15 mm wide gaps between timber planks
Testing arrangement	Steel samples and sensors were installed at six locations as shown in Figure 72
Monitoring period	1 August 2013 to 4 August 2014

Figure 70. House 5 exterior.


Figure 71. House 5 subfloor.
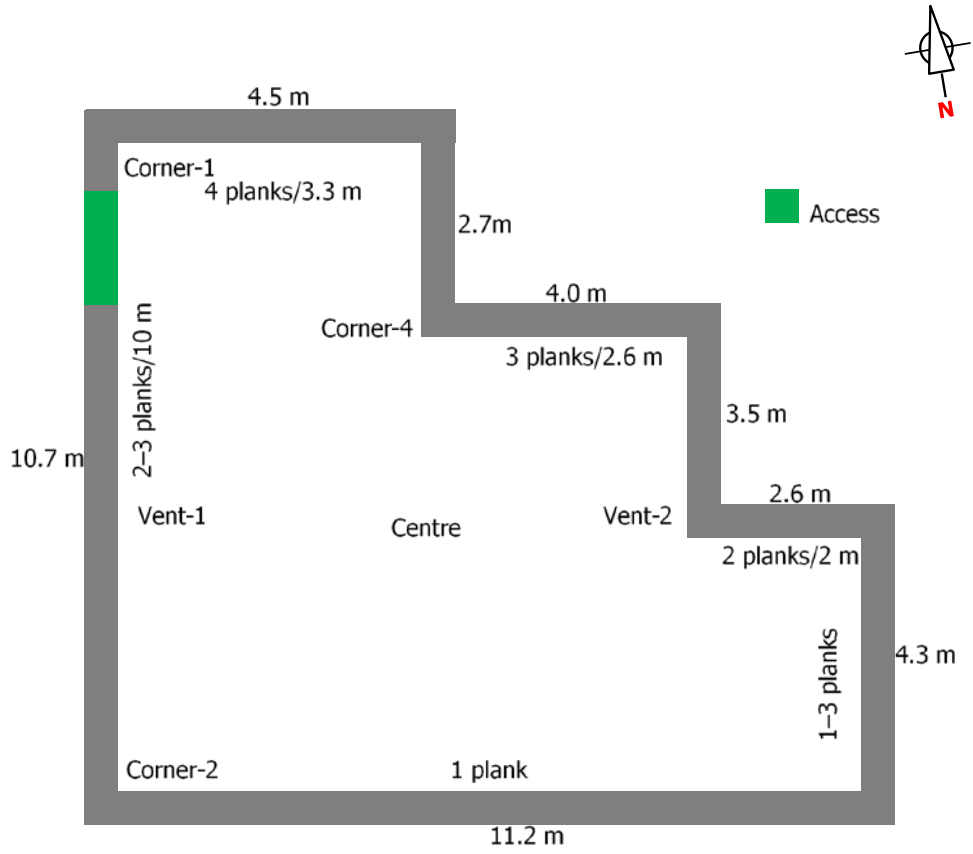
Figure 72. Dimensions of subfloor and sample arrangement of house 5.

A.6 House 6 – Wellington

Construction	Concrete corner with timber planks, weatherboards – see Figure 73 and Figure 74
Underfloor insulation	R1.5 polyester
Subfloor ground	Not covered but appeared to be dry
Configuration/dimensions	See Figure 75
Ventilation	~25 mm wide gaps between timber planks
Testing arrangement	Steel samples and sensors were installed at seven locations as shown in Figure 75
Monitoring period	3 August 2013 to 4 August 2014

**Figure 73. House 6 exterior.**

Figure 74. House 6 subfloor.
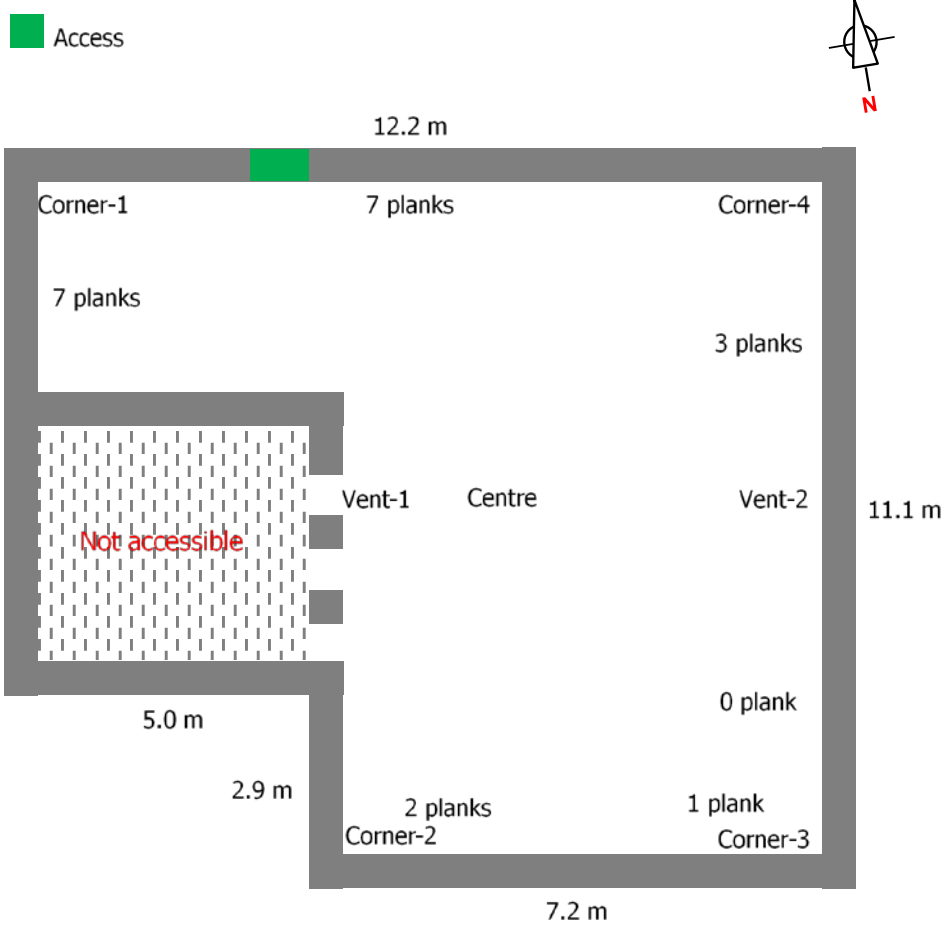
Figure 75. Dimensions of subfloor and sample arrangement of house 6.

A.7 House 7 – Invercargill

| Construction	Concrete
Underfloor insulation	No insulation – see Figure 76
Subfloor ground	No ground covered and soil relatively wet
Configuration/dimensions	See Figure 77
Ventilation	~14 vents with a dimension of 130 × 200 mm – each has 10 holes of 80 × 10 mm
Testing arrangement	Steel samples and sensors were installed at seven locations as shown in Figure 77
Monitoring period	20 July 2013 to 19 July 2014

Figure 76. House 7 subfloor.
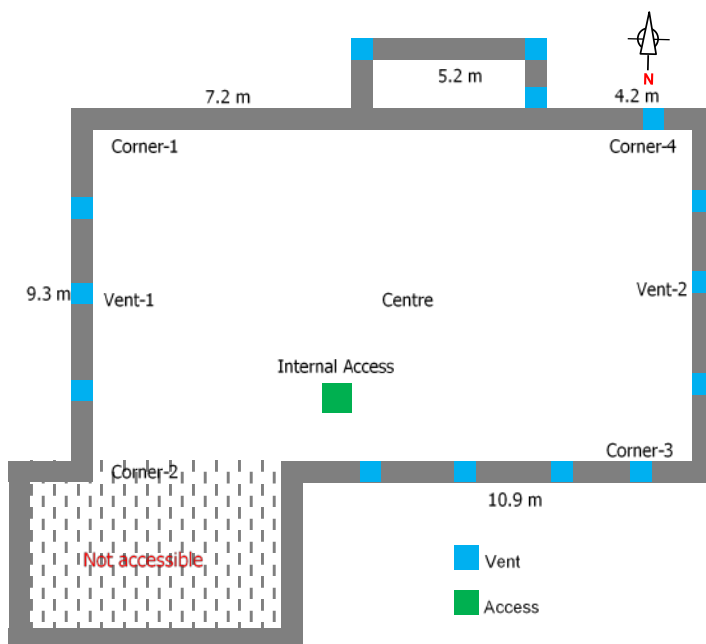
Figure 77. Dimensions of subfloor and sample arrangement of house 7.

65

A.8 House 8 – Invercargill

Construction	Concrete perimeter foundation wall, brick veneer wall cladding – see Figure 78 and Figure 79
Underfloor insulation	No insulation
Subfloor ground	No ground covered, soil relatively wet on some parts while other parts appears to be relatively dry
Configuration/dimensions	See Figure 80
Ventilation	~20 vents with a dimension of 300 × 130 mm – each has 40 holes of 20 × 20 mm
Testing arrangement	Steel samples and sensors were installed at six locations as shown in Figure 80
Monitoring period	20 July 2013 to 20 July 2014

**Figure 78. House 8 exterior.**

Figure 79. House 8 subfloor.
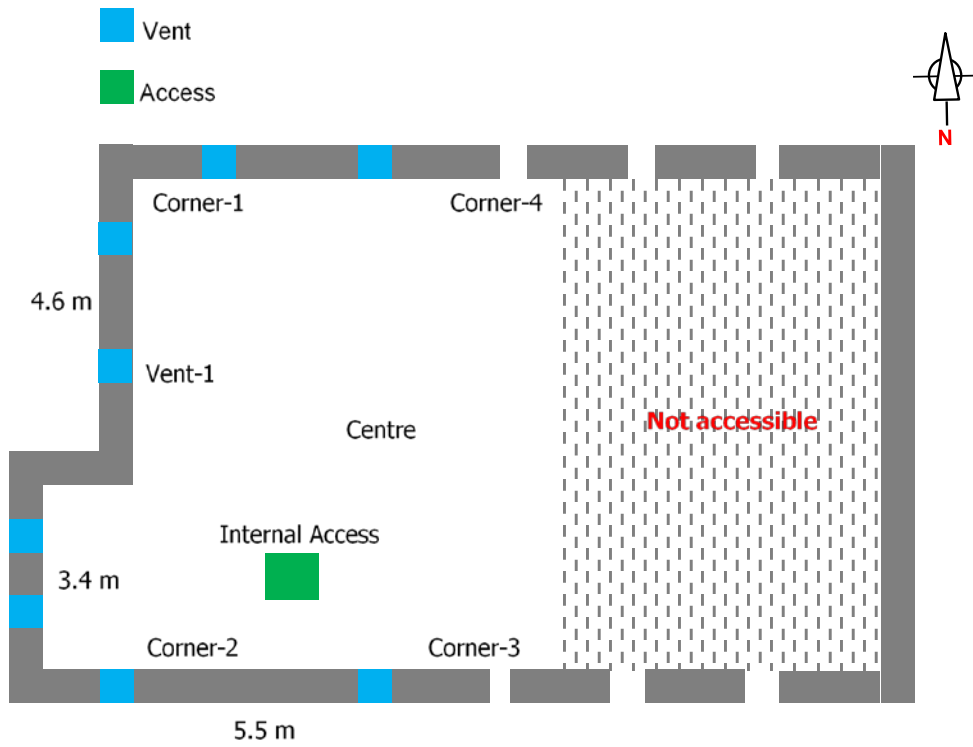
Figure 80. Dimensions of subfloor and sample arrangement of house 8.